Available online at www.sciencedirect.com
SCIENCE DIRECT®
Geochimica et Cosmochimica Acta 70 (2006) 2191–2209
Geochimica
www.elsevier.com/locate/gca

The effects of organic acids on the dissolution of silicate minerals: A case study of oxalate catalysis of kaolinite dissolution

Jordi Cama [1], Jiwchar Ganor *

Department of Geological and Environmental Sciences, Ben-Gurion University of the Negev, P.O. Box 653, Beer-Sheva 84105, Israel

Received 17 December 2004; accepted in revised form 30 January 2006

Abstract

Most studies agree that the dissolution rate of aluminosilicates in the presence of oxalic and other simple carboxylic acids is faster than the rate with non-organic acid under the same pH. However, the mechanisms by which organic ligands enhance the dissolution of minerals are in debate. The main goal of this paper was to study the mechanism that controls the dissolution rate of kaolinite in the presence of oxalate under far from equilibrium conditions ($-29 < \Delta G_r < -18$ kcal mol^{-1}). Two types of experiments were performed: non-stirred flow-through dissolution experiments and batch type adsorption isotherms. All the experiments were conducted at pH 2.5–3.5 in a thermostatic water-bath held at a constant temperature of 25.0, 50.0 or 70.0 ± 0.1 °C. Kaolinite dissolution rates were obtained based on the release of silicon and aluminum at steady state. The results show good agreement between these two estimates of kaolinite dissolution rate. At constant temperature, there is a general trend of increase in the overall dissolution rate as a function of the total concentration of oxalate in solution. The overall kaolinite dissolution rates in the presence of oxalate was up to 30 times faster than the dissolution rate of kaolinite at the same temperature and pH without oxalate as was observed in our previous study. Therefore, these rate differences are related to differences in oxalate and aluminum concentrations. Within the experimental variability, the oxalate adsorption at 25, 50, and 70 °C showed the same dependence on the sum of the activities of oxalate and bioxalate in solution. The change of oxalate concentration on the kaolinite surface ($C_{s,ox}$) as a function of the sum of the activities of the oxalate and bioxalate in solution may be described by the general adsorption isotherm:

$$C_{s,ox} = 6.1 \times 10^{-7} \cdot \frac{64 \cdot \left(a_{HC_2O_4^-} + a_{C_2O_4^{2-}}\right)^{0.48}}{1 + 64 \cdot \left(a_{HC_2O_4^-} + a_{C_2O_4^{2-}}\right)^{0.48}}.$$

The possible effect of oxalate on the proton-promoted dissolution rate was examined by comparing the results of the present study to literature observations on the effects on kaolinite dissolution rate of deviation from equilibrium and Al inhibition, respectively. The comparison indicates that the effect of oxalate on kaolinite dissolution rate is not related to Al inhibition or saturation state. Therefore, we suggest that oxalate catalyzes kaolinite dissolution through an oxalate-specific mechanism. The oxalate-promoted dissolution is best described using a quadratic rate law, i.e., a rate law in which the oxalate-promoted dissolution rate depends on the square of the oxalate surface concentration. A quadratic rate law may represent a mechanism in which the dissolution is catalyzed by the simultaneous adsorption of two ligands on two neighboring edge aluminol sites. This mechanism is supported by the observation that on saturation, the amount of adsorbed oxalate is similar to the amount of available Al surface sites on the kaolinite edge, and is much smaller than the amount of available Al surface sites on the basal planes. This observation indicates that the adsorption of oxalate occurs mainly on edge

* Corresponding author. Fax: +972 8 6472 997.
E-mail address: ganor@bgu.ac.il (J. Ganor).
URL: http://www.bgu.ac.il/geol/ganor/ (J. Ganor).
[1] Present address: Department of Environmental Geology, Institute of Earth Sciences "Jaume Almera", CSIC, Lluís Solé i Sabarís s/n, Barcelona 08028, Catalonia (Spain).

0016-7037/$ - see front matter
doi:10.1016/j.gca.2006.01.028

aluminol sites, and suggests that the formation of Al-oxalate complexes on two neighboring edge aluminol sites must be reasonably common above a threshold oxalate concentration.

1. Introduction

1.1. General rate law of dissolution reactions

A general form of rate law for one mechanism of heterogeneous mineral surface reactions can be written as (Lasaga, 1998):

$$\text{Rate} = k_0 \cdot S_a \cdot e^{-E_a/RT} \cdot a_{H^+}^{n_{H^+}} \cdot \prod_i a_i^{n_i} \cdot g(I) \cdot f(\Delta G), \quad (1)$$

where k_0 is a constant, S_a is the reactive surface area of the mineral, E_a is the apparent activation energy of the overall reaction, R is the gas constant, T is the temperature (K), a_i and a_{H^+} are the activities in solution of species i and H^+, respectively, n_i and n_{H^+} are the orders of the reaction with respect to these species, $g(I)$ is a function of the ionic strength, and $f(\Delta G)$ is a function of the Gibbs free energy. The much-studied pH dependence of the dissolution/precipitation reactions is represented by the term $a_{H^+}^{n_{H^+}}$ in Eq. (1). Terms involving activities of species in solution other than H^+, $a_i^{n_i}$, incorporate other possible catalytic effects on the overall rate. The $g(I)$ term indicates a possible dependence of the rate on the ionic strength (I) in addition to that entering through the activities of a specific ion. The last term, $f(\Delta G)$, accounts for the important variation of the rate with deviation from equilibrium. The role of inhibition is not described in Eq. (1). Depending on the exact inhibition mechanism, the term a_i may represent an inhibitor. However, commonly this is not the case, and other terms should be introduced into the equation (see, for example, Eqs. (14) and (43) of Ganor and Lasaga, 1998; Eqs. (7.78) and (7.79) of Lasaga, 1998; and Eq. (44) of Ganor et al., 1999). In some of these inhibition mechanisms, competition takes place and the general rate law cannot be described by a product of independent terms.

The formulation of Eq. (1) is very useful because it relates the reaction rate to activities of ions in solution that may be obtained directly from the chemistry of the solution. However, mineral dissolution is a surface process and therefore it is more appropriate to express the dependence of the rate on the concentrations (or activities) of ions adsorbed on the surface rather than on the bulk activities in solution. Therefore, Eq. (1) can be rewritten in terms of surface concentrations ($X_{i,ads}$):

$$\text{Rate} = k_0 \cdot S_a \cdot e^{-E_a/RT} \cdot X_{H^+,ads}^{n_{H^+,ads}} \cdot \prod_i X_{i,ads}^{n_{i,ads}} \cdot g(I) \cdot f(\Delta G). \quad (2)$$

The coefficients $n_{H^+,ads}$ and $n_{i,ads}$ are the reaction orders with respect to the surface species. Eqs. (1) and (2) describe a general rate law for *one mechanism*. The overall rate of a reaction is the sum of the rates of all mechanisms involved.

1.2. Previous studies on the catalytic effects of oxalate on dissolution reactions

The effects of organic acids on weathering of minerals have been the subject of scientific discussions for several decades. The focus of these discussions has been on three major questions: first, is the dissolution rate faster in the presence of organic acid than in the presence of non-organic acid under the same pH? Second, to what extent do organic acids affect mineral dissolution rates under natural conditions? Third, what is the mechanism that is responsible for the enhancement of dissolution rate in the presence of organic acids? The results of some of these studies were summarized by Bennett and Casey (1994), Drever and Vance (1994), Hajash (1994), Stillings et al. (1996), Drever and Stillings (1997), Stillings et al. (1998), Oelkers and Schott (1998), Blake and Walter (1999), and van Hees et al. (2002). For oxalic acid, most of the studies agree that the answer to the first question is positive (e.g., Stillings et al., 1998). The second and the third questions are still the subject of scientific debates.

An important benchmark in the discussion of the third question was the work of Furrer and Stumm (1986) on the catalytic effect of both dicarboxylic and aromatic acids on the dissolution of oxides. They proposed a detailed surface-controlled reaction mechanism, in which the overall dissolution rate in the presence of organic ligand is the sum of the rates of two independent surface reaction mechanisms: the proton-promoted and the ligand-promoted mechanisms. Furrer and Stumm (1986) suggested that the ligand-promoted dissolution rate is linearly proportional to the surface concentration of the respective adsorbed ligand. A considerable volume of work assessing the catalytic effect of organic acids on silicate dissolution has been carried out since this work of Furrer and Stumm (1986). Most of these studies have focused on feldspar (Welch and Ullman, 1993; Franklin et al., 1994; Blake and Walter, 1996; Stillings et al., 1996; Welch and Ullman, 1996; Drever and Stillings, 1997; Stillings et al., 1998; Blake and Walter, 1999; van Hees et al., 2002). The effect of organic acids on kaolinite was studied by Chin and Mills (1991), Wieland and Stumm (1992), and Ganor and Lasaga (1994). Following Furrer and Stumm (1986), all the abovementioned studies on kaolinite dissolution expressed the overall dissolution rate as the sum of proton-promoted rate and ligand-promoted rate. Chin and Mills (1991) studied the effect of low-molecular-weight organic acids on the kaolinite dissolution rate under acidic conditions, and found that Al was

released faster than Si. Wieland and Stumm (1992) and Ganor and Lasaga (1994) obtained stoichiometric dissolution of kaolinite in the presence of oxalate. Chin and Mills (1991) observed a linear dependency of the oxalate-promoted rate on the surface concentration of oxalate. Ganor and Lasaga (1994) observed that the oxalate-promoted rate has a non-linear dependency on the concentration of bioxalate in solution. They calculated that the reaction order with respect to $a_{HC_2O_4^-}$ is 0.30 ± 0.01.

Drever and Stillings (1997) reviewed the effect of low-molecular-weight organic acids on dissolution, and concluded that: (1) small ligands such as oxalate appear to accelerate feldspar dissolution through complexation of Al at the surface of the mineral; (2) in general, oxalate concentrations of the order of 1 mM are necessary to cause a significant effect; and (3) in nature, the effect of complexation of dissolved Al on the dissolution rate of silicate does not appear to be significant. It is important to note that the environmental conditions in the field and the degree of complexity are very different from those in laboratory experiments. Therefore, extrapolation from laboratory experiments to field conditions requires a thorough understanding of the reaction mechanism.

A simple ligand-promoted reaction mechanism consists of fast adsorption of the organic ion on the mineral surface followed by a slow catalyst-mediated hydrolysis step, which is the rate-determining step. The rate of the hydrolysis depends on the adsorbed surface species. Therefore, the rate law must include the adsorption isotherms of the organic ion. However, only a few studies on the effect of organic acids on silicate dissolution have measured the adsorption isotherm (e.g., Stillings et al., 1998). Ward and Brady (1998) carried out adsorption measurements of oxalate on kaolinite at 25 and 60 °C from pH 2 to 12. They showed that oxalate adsorption is stronger than acetate and formate adsorption at near neutral and acidic pH. Poulson et al. (1997) found that oxalate adsorption onto quartz surfaces is negligible. They re-evaluated the quartz dissolution rate data and suggested that oxalate per se has little or no effect upon quartz dissolution. Oelkers and Schott (1998) argue that the observed enhancement of alkali-feldspar dissolution rates by the presence of organic acids is a result of the decrease in Al^{3+} activity due to aqueous aluminum–organic acid anion complex formation. They suggest that organic anion surface adsorption, if it does occur, has a negligible effect on alkali-feldspar dissolution rates. On the other hand, Stillings et al. (1998) measured oxalate adsorption on the surface of andesine and found that the surface complexation model is fully consistent with the effect of oxalate on andesine dissolution rate. Stillings et al. (1998) noted that this explanation is not necessarily unique, and more detailed information on the behavior of adsorbed oxalate on the molecular level and on the detachment of atoms during the dissolution of feldspar is necessary in order to test the model.

After all these studies the mechanisms by which organic ligands enhance the dissolution of minerals are in debate (compare, for example, Oelkers and Schott, 1998; Stillings et al., 1998). The focus of the debate has been whether the observed enhancement of the overall dissolution rate is the result of an enhancement of the rate of proton-promoted dissolution (through an effect of oxalate on Al speciation in solution, which affects both the Al inhibition and the overall saturation state), or whether an inner-sphere oxalate adsorption complex facilitates the detachment of metal ions and thus enhances the dissolution rate (Stumm, 1992).

1.3. The goal of the present study

The aim of the present paper was to study the effect of oxalate on both the proton-promoted and the oxalate-promoted dissolution of kaolinite, and to assess which of the two possible mechanisms is dominant in enhancing kaolinite dissolution under acidic conditions in the presence of oxalate. We have chosen to study the effect of oxalate on kaolinite for the following reasons: (1) kaolinite is a simple, common aluminosilicate mineral; (2) the proton-promoted dissolution of kaolinite in general and the effects of temperature, pH and Al in particular have been thoroughly studied (Carroll-Webb and Walther, 1988; Carroll and Walther, 1990; Chin and Mills, 1991; Nagy et al., 1991; Wieland and Stumm, 1992; Xie and Walther, 1992; Ganor et al., 1995; Devidal et al., 1997; Huertas et al., 1999; Metz and Ganor, 2001; Cama et al., 2002); (3) oxalic acid is a simple carboxylic acid that is relatively abundant in soil and groundwater, with concentrations ranging from 10^{-5} to 10^{-3} M in upper soil horizons (Graustein et al., 1977; Fox and Comerford, 1990; Crossey, 1991); (4) thermodynamic data on the speciation of oxalate at different temperatures, some thermodynamic data on their complexes with Al in solution, and kinetic data on the rate of decomposition of this organic acid are available (see Harrison and Thyne, 1992; Bell and Palmer, 1994; Bell et al., 1994; Harrison and Thyne, 1994; Ganor et al., 2001, for details and references); (5) there are some preliminary data on the adsorption of oxalate on kaolinite and on the effect of oxalate on kaolinite dissolution (Chin and Mills, 1991; Wieland and Stumm, 1992; Ganor and Lasaga, 1994; Ward and Brady, 1998; Ganor et al., 2001). In order to keep the proton-promoted dissolution rate constant and under far from equilibrium conditions, we performed all the experiments at pH from 2.5 to 3.5. The study was carried out at temperatures of 25, 50, and 70 °C to quantify the temperature effect.

We performed two types of experiments: (1) batch experiments to determine the adsorption isotherms of oxalate on the kaolinite surface; and (2) non-stirred flow-through experiments to measure the kinetics of kaolinite dissolution. We chose to conduct non-stirred experiments for two reasons. First, for slow reactions such as kaolinite dissolution, there is little likelihood of diffusion control in a flowing, albeit non-stirred, reactor system (e.g., Ganor and

Metz, 2001; Metz and Ganor, 2001). Even though kaolinite dissolution is a surface-controlled reaction, stirring of kaolinite affects the dependence of its dissolution rate on kinetic factors (e.g., pH, temperature, activation energy, and degree of saturation). Metz and Ganor (2001) explained this stirring effect by the formation of very fine kaolinite particles as a result of spalling-off or abrasion of the kaolinite. These very fine particles have a very high ratio of reactive surface area to specific surface area and therefore, the dissolution rate increased with stirring. Second, use of the non-stirred system allows us to most directly compare the results presented here with those of Cama et al. (2002) on the effect of Al and pH on kaolinite dissolution rate, which were conducted at the same temperatures using non-stirred reactors.

2. Materials and methods

2.1. Characterization and pretreatment of kaolinite

The kaolinite samples used in this study, KGa-1 and KGa-1B, are international reference samples of the Clay Mineral Society Source Clay Repository. To obtain stoichiometric dissolution raw kaolinite samples have been pretreated (Nagy et al., 1991). Sample KGa-1 was pretreated in 0.001 N $HClO_4$ at 80 °C for a few months using the procedure described by Ganor et al. (1995). Sample KGa-1B was pretreated in 0.001 N HNO_3 at 70 °C using a similar procedure.

Samples were degassed in a N_2 atmosphere for 48 h at 135 °C. Afterwards, surface area was measured using 5-point N_2 adsorption isotherms with a Micromeritics Gemini 2370 surface area analyzer. The BET-determined initial surface area of pretreated KGa-1, untreated KGa-1B, and pretreated KGa-1B were 8.1 ± 0.2, 10.5 ± 0.3, and 10.9 ± 0.3 $m^2\ g^{-1}$, respectively.

2.2. Experimental setting

2.2.1. Flow-through dissolution experiments

Dissolution experiments were carried out using non-stirred flow-through reactors (ca. 35 ml in volume) fully immersed in a thermostatic water-bath held at a constant temperature of 25.0, 50.0 or 70.0 ± 0.1 °C. The reaction cells were composed of two chambers, a lower chamber of 33-mm inner diameter and an upper chamber of 26-mm inner diameter. The two chambers were separated by a fine (5 μm) nylon mesh, on which kaolinite powder was placed. A schematic sketch of the experimental setting and some more details of the experimental procedure can be found in Metz and Ganor (2001) and Amram and Ganor (2005).

2.2.2. Adsorption measurements

Oxalate adsorption to kaolinite was determined in polyethylene batch reactors fully submersed in a thermostatic water-bath held at a constant temperature of 25.0, 50.0 or 70.0 ± 0.1 °C. Variable amounts of kaolinite and of mixed solution of HNO_3 and oxalate were placed for 2 h in the reactor. This duration was found to be sufficient for equilibration between the oxalate in solution and the kaolinite surface (Ganor et al., 2001). In some of the experiments, the samples were vigorously shaken during the first 30 s of the experiment, and left unstirred thereafter. In the other experiments, the samples were mixed using a magnetic stirrer during the entire span of the experiment. Prior to the experiments at 50 and 70 °C the dry kaolinite was heated inside a furnace to the respective temperature. All the suspensions were magnet-stirred for 15 min and closed to avoid evaporation. After equilibration, the suspension was allowed to settle for a short time. Most of the suspended material was introduced into a syringe and filtered through a Whatman 0.45 μm polyvinylidene fluoride (PVDF) 13 mm syringe filter and stored in a clean polyethylene bottle. The recovered kaolinite powder was washed through a Millipore 0.45 μm filter, dried, weighed, and its surface area was measured.

2.2.3. Solutions and analyses

Solutions were prepared by mixing reagent grade 1 M HNO_3, 0.01 M $Na_2(COO)_2$, and double deionized water (DDW). In several cases, adequate quantities of $AlCl_3$ standard solution (1000 ppm, Merck) were added into the solution to obtain Al-rich solutions. An antibiotic mixture was added to several of the solutions using a 1/100 volumetric ratio. The antibiotic mixture is prepared by dissolving 100-mg penicillin-G, 50-mg streptomycin, 50-mg ampicillin, and 20-mg chloramphenicol (all from Sigma) in 10 ml DDW.

The concentration of oxalate was measured using a Dionex DX-500 Chromatography System with an IonPac AS4A-SC column. Eluent solutions of 32 mM NaOH were prepared from reagent grade sodium hydroxide 50% (w/w) solution (Baker). The uncertainty in measured oxalate is usually better than ±1% for concentrations above 25 μM. The precision drops to ±10% and 15% for measurements below 25 and 5 μM, respectively. Al-rich (up to 400 μM) oxalate standard solutions were analyzed to verify that the measurement of total oxalate was not influenced by the presence of Al-oxalate complexes. Indeed, the complexes did not interfere with the measurement and the total oxalate concentration was accurately determined. Total Si was analyzed colorimetrically with a UV–visible spectrophotometer, using the molybdate blue method (Koroleff, 1976). The uncertainty in measured Si was better than ±5% for concentrations above 4 μM. The precision dropped to ±15% and 33% for measurements at low concentrations of 2 and 0.5 μM, respectively. Total Al was analyzed by Inductively Coupled Plasma Atomic Emission Spectroscopy (ICP-AES, Perkin-Elmer 3000). The uncertainty in ICP-AES measurements was better than ±5%. The pH was measured at experimental temperature on an unstirred aliquot of solution using a semi-micro 83-01 Orion Ross combination

electrode. The reported accuracy is ±0.02 pH units (±4.5% in H^+ activities).

3. Calculations

3.1. Kaolinite dissolution rate

The overall dissolution reaction of kaolinite under acidic conditions can be expressed as:

$$Al_2Si_2O_5(OH)_4 + 6H^+ \rightarrow 2Al^{3+} + 2H_4SiO_4 + H_2O \quad (3)$$

The dissolution rate, Rate (mol m^{-2} s^{-1}), in steady state was based on the release of Al and Si according to the expression:

$$v_j \cdot \text{Rate} = -\frac{q}{A}(C_{j,\text{out}} - C_{j,\text{inp}}), \quad (4)$$

where $C_{j,\text{inp}}$ and $C_{j,\text{out}}$ are the concentrations of component j (Al or Si) in the input and the output solutions, respectively (mol m^{-3}), v_j is the stoichiometry coefficient of j in the dissolution reaction, A is the surface area (m^2), and q is the fluid volume flux through the system (m^3 s^{-1}). Note that in our formalism, the rate is defined to be negative for dissolution and positive for precipitation. The error in the calculated rate (ΔRate) is estimated using the Gaussian error propagation method (Barrante, 1974) from the equation:

$$\Delta P = \left[\sum_i \left(\frac{\partial P}{\partial x_i}\right)^2 (\Delta x_i^2)\right]^{1/2}, \quad (5)$$

where P is the calculated parameter (Rate in Eq. (4)) and Δx_i is the estimated uncertainty of the measurements of the quantity x_i, which is used in the calculation of the parameter (e.g., q and A in Eq. (4)). For most of the experiments, the error in the calculated rate ranged from 14% to 24%.

3.2. Speciation in solution and degree of saturation

The speciation of ions in solution and the solution saturation state were calculated using the DELGORG computer code (Ganor, unpublished), as follows: The distributions of Al, Si, and oxalate aqueous species were calculated using appropriate thermodynamic data (Table 1). Activity coefficients were calculated using the extended Debye–Huckel equation with parameters from Wolery (1979). The degree of saturation of the solution with respect to kaolinite dissolution (Eq. (3)) is calculated in terms of the Gibbs free energy of reaction ΔG_r

$$\Delta G_r = RT \ln\left(\frac{\text{IAP}}{K_{eq}}\right) = RT \ln\left(\frac{a_{Al^{3+}}^2 \cdot a_{H_4SiO_4}^2}{a_{H^+}^6 \cdot K_{eq}}\right), \quad (6)$$

where R is the gas constant, T is the absolute temperature, IAP is the ion activity product of the solution, and K_{eq} is the solubility constant. Errors in IAP and ΔG_r were estimated according to the Gaussian error propagation method (Barrante, 1974) using Eq. (5).

3.3. Adsorption of oxalate on kaolinite surface

The concentration of oxalate surface complexes is determined by subtracting the oxalate concentration of the solution after equilibration from the initial concentration:

$$C_s = (C_{f,i} - C_{f,e}) \cdot \frac{V}{A}, \quad (7)$$

where C_s is the concentration of the oxalate surface complexes (mol m^{-2}), $C_{f,i}$ and $C_{f,e}$ are the initial and equilibri-

Table 1
Equilibrium constant ($\log K_{eq}$) used in the calculations

Reaction	25 °C	50 °C	80 °C	Reference
$Al^{3+} + OH^- = Al(OH)^{+2}$	9.0	9.1	9.1	1
$Al^{3+} + 2OH^- = Al(OH)_2^+$	17.4	17.3	17.4	1
$Al^{3+} + 3OH^- = Al(OH)_3$	24.6	24.8	25.0	1
$Al^{3+} + 4OH^- = Al(OH)_4^-$	33.0	32.6	32.5	1
$Al^{3+} + C_2O_4^{-2} = AlC_2O_4^+$	7.1	8.7	10.1	2
$Al^{3+} + 2C_2O_4^{-2} = Al(C_2O_4)_2^-$	13.0	14.6	16.0	3
$Al^{3+} + 3C_2O_4^{-2} = Al(C_2O_4)_3^{-3}$	16.3	17.9	19.3	3
$H_2C_2O_4 = 2H^+ + C_2O_4^{-2}$	−4.3	−4.4	−4.5	4
$HC_2O_4^- = H^+ + C_2O_4^{-2}$	−5.5	−5.8	−6.0	4
$H^+ + OH^- = H_2O$	−14.0	−13.3	−12.8	5
$H_4SiO_4 = H_3SiO_4^- + H^+$	−9.7	−9.3	−9.1	6
Kaolinite dissolution (Eq. (1))	8.9	6.4	4.6	7

[1]Wesolowski and Palmer (1994).
[2]Calculated using a linear fit to the data of Harrison and Thyne (1992) at 0, 25, 60, 100, 150, and 200 °C.
[3]25 °C constant is from Graustein (1981). The constants at 50 and 70 °C were calculated assuming that the slope is the same as that of $AlC_2O_4^+$. The intercept was calculated using the 25 °C constant of Graustein (1981).
[4]Kettler et al. (1991).
[5]Busey and Mesmer (1978).
[6]Equilibrium constants were obtained from standard state thermodynamic data of Naumov et al. (1974).
[7]Equilibrium constants were obtained from standard state thermodynamic data, calculated from K_{eq} at 80 °C of Nagy et al. (1991).

um concentrations of the fluid (mol m^{-3}), respectively, V is the fluid volume (m^3), and A is the total surface area (m^2).

The error in the calculated surface concentration (ΔC_s) was estimated using a Gaussian error propagation method (Barrante, 1974) from the equation:

$$\Delta C_s = \sqrt{\left(\frac{V}{A}\right)^2 \cdot (\Delta C_{f,i}^2 + \Delta C_{f,e}^2) + \left(\frac{C_{f,i} - C_{f,e}}{A}\right)^2 \cdot \Delta V^2 + \left(\frac{C_{f,i} - C_{f,e}}{A^2} \cdot V\right)^2 \cdot \Delta A^2}. \quad (8)$$

The errors in the calculated surface concentration include the uncertainty of the volume (ΔV), uncertainty of the surface area (ΔA), and the uncertainty of the oxalate measurements ($\Delta C_{f,i}$ and $\Delta C_{f,e}$).

The above calculation is based on the observations of Ganor et al. (2001) that oxalate decomposition is negligible during the short period of the adsorption experiments, and that oxalate is not consumed by any other processes.

4. Results

4.1. Flow-through experiments

The variations with time of the input and the output oxalate concentrations and of the Si concentration in a representative flow-through experiment are shown in Fig. 1. This experiment was composed of five stages, in which each new stage was initiated by a change in the flow rate, temperature, and/or the composition of the input solution. The vertical lines in the figure delineate the different stages. The system response to changes in the experimental conditions was very fast, and the system approaches a new steady state within first or second sampling after each change. Much of the variability in the non-steady-state data results from instabilities in flow rate. The experimental conditions of all experiments are compiled in Table 2. Duration of steady state varies but mostly surpasses 300 h. Several studies (e.g., Walther, 1996; Gautier et al., 2001) indicated that the amount of time prior to steady state may influence the resulting steady-state dissolution rate. Fig. 1 shows the

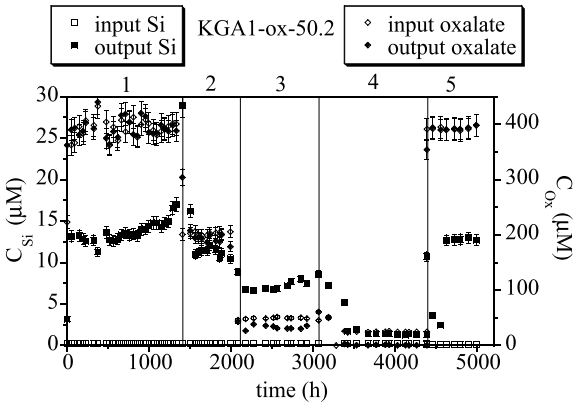

Fig. 1. Variation in oxalate and Si concentration as a function of time in a representative experiment. The vertical lines represent changes in experimental conditions between the different stages.

change in Si concentration in a multi-stage experiment (KGA1-50-ox-2) in which both oxalate concentration and temperature varied between the stages. The temperature was maintained at 50 °C in stages 1–3, dropped to 25 °C in stage 4, and returned to 50 °C in the last stage, 5. The experiment attained the first steady state, at 50 °C and oxalate concentration of 400 μM, after 900 h. The dissolution rate at steady state in stage 1 was $1.0 \pm 0.2 \times 10^{-12}$ mol m^{-2} s^{-1}. After more than 3000 h under variable experimental conditions, temperature and input oxalate were changed back to 50 °C and 400 μM, respectively, and a new steady state (5) was achieved. The dissolution rate at this last steady state was $1.1 \pm 0.2 \times 10^{-12}$ mol m^{-2} s^{-1}, which is (within error) the same dissolution rate as that of stage 1.

Kaolinite dissolution rates (Eq. (4)) were obtained based on the release of silicon ($Rate_{Si}$) and aluminum ($Rate_{Al}$) at steady state, for each flow-through experiment (Table 2). Fig. 2 plots the dissolution rates evaluated based on the release of Si versus those obtained based on the release of Al. The solid lines in Fig. 2 are the 1/1 diagonal. Taking into account the appropriate errors, Fig. 2 shows a good agreement between the different estimates of kaolinite dissolution rate. To minimize errors, dissolution rate was calculated as the average of $Rate_{Al}$ and $Rate_{Si}$ in all experiments in which the error associated with both is less than 25% (Table 2). In the rest of the experiments, we used either $Rate_{Al}$ or $Rate_{Si}$, whichever had the smaller error.

The overall kaolinite dissolution rate was up to 30 times faster in the presence of oxalate than the dissolution rate of kaolinite at the same temperature and pH without oxalate. The data on dissolution rates without oxalate were taken from Cama et al. (2002). In the present study, we used the same batch of kaolinite sample and the same experimental setting as in the study of Cama et al. (2002). Therefore, the rate differences between the experiments are related to differences in oxalate and aluminum concentrations. Fig. 3 plots the overall kaolinite dissolution rate as a function of the total concentration of oxalate. At constant temperature, there is a general trend of an increase in the overall dissolution rate as a function of the total concentration of oxalate in solution, i.e., the sum of oxalate in all the complexes in solution.

4.2. Adsorption experiments

Initial and final oxalate concentrations in solution are compiled in Table 3. Final oxalate concentrations ranged from 0 to 7 mM. The final concentration of the oxalate was not influenced by the addition of an antibiotic mixture to the initial solution. Blank experiments (with no mineral) were conducted to verify that the oxalate was not adsorbed by the reactor walls nor affected by the extraction and filtration processes. No significant change in solution composition was observed in the blank experiments, and therefore we suggest that the decrease in oxalate concentration is a result of oxalate adsorption on the kaolinite surface. The

Table 2
Experimental conditions and steady-state average concentration of the flow-through experiments

Experiment[a]	T (°C)	Flow rate (ml min^{-1})	pH		[oxalate] (μM)		[Si] (μM)		[Al] (μM)		Steady state			$Rate_{Si}$[d] (mol m^{-2} s^{-1})	$\Delta Rate_{si}$[e] (%)	$Rate_{Al}$[d] (mol m^{-2} s^{-1})	$\Delta Rate_{Al}$[e] (%)	Ionic strength (M)	ΔG_r (kcal mol^{-1})
			Input	Output	Input	Output	Input	Output	Input	Output	Al/Si[b]	Mass[c] (g)	Area[c] (m^2 g^{-1})						
KGA1-ox-50.1.2	25	0.037	3.23	3.29	396	341	0.28	0.97	0.50	1.2	1.05	0.25	8.6	−9.9E−14	107	−1.8E−13	92	0.002	−28.8
KGA1-ox-50.3.4	25	0.031	3.36	3.33	387	308	0.28	2.45	0.00	2.3	1.06	1.01	8.6	−6.5E−14	65	−6.9E−14	57	0.001	−26.6
KGA1-ox-50.3.5	25	0.036	3.10	3.15	207	136	0.10	2.22	0.00	nd		1.01	8.6	−7.3E−14	60			0.001	−25.4
KGA1-ox-25.7.4	25	0.012	2.74	2.88	1421	1017	0.23	12.93	0.50	17	1.34	1.01	8.0	−1.6E−13	21	−2.4E−13	20	0.005	−26.3
KGA1-ox-25.7.5-ANB	25	0.012	2.98	2.92	979	1018	0.23	12.39	0.50	15	1.15	1.01	8.0	−1.5E−13	21	−1.8E−13	21	0.004	−26.5
KGA1-ox-25.7.6	25	0.012	2.82	2.90	1008	705	0.23	9.16	0.50	10	1.06	1.00	8.0	−1.1E−13	21	−1.3E−13	21	0.004	−26.5
KGA1-ox-50.1.3	50	0.035	3.11	3.13	202	192	0.28	7.78	0.00	nd		0.25	8.6	−1.0E−12	21			0.001	−25.5
KGA1-ox-50.1.4	50	0.035	2.98	2.98	50	32	0.28	4.80	0.50	5	0.99	0.25	8.6	−6.3E−13	22	−6.9E−13	24	0.001	−23.2
KGA1-ox-50.2.1	50	0.037	3.24	3.24	394	397	0.28	14.43	0.10	14	0.95	0.50	8.5	−1.0E−12	21	−1.0E−12	21	0.002	−25.5
KGA1-ox-50.2.2	50	0.036	3.12	3.14	201	194	0.28	11.53	0.00	9	0.78	0.49	8.5	−8.0E−13	21	−6.3E−13	21	0.001	−24.8
KGA1-ox-50.2.3	50	0.037	2.98	3.08	50	32	0.28	7.26	0.00	nd		0.49	8.5	−5.1E−13	22			0.001	−21.4
KGA1-ox-50.2.5	50	0.042	3.23	3.23	392	393	0.10	12.79	0.00	14	1.12	0.49	8.5	−1.1E−12	21	−1.2E−12	21	0.002	−25.0
KGA1-ox-50.3.1	50	0.037	3.24	3.28	394	391	0.28	24.28	0.20	26	1.07	1.02	8.6	−8.4E−13	21	−9.2E−13	21	0.002	−23.6
KGA1-ox-50.3.6	50	0.037	2.71	2.77	1424	1411	0.10	49.90	0.00	50	1.01	1.00	8.6	−1.8E−12	21	−1.8E−12	21	0.006	−26.9
KGA1-ox-50.3B.7	50	0.044	3.56	3.52	1445	1440	0.10	28.39	0.00	nd		1.00	8.6	−1.2E−12	21			0.005	−26.4
KGA1B-ox-70.1.1	70	0.043	3.12	3.19	211	123	0.69	25.96	0.20	26	1.02	0.20	13.2	−3.5E−12	21	−3.6E−12	21	0.001	−22.1
KGA1B-ox-70.1.2.2	70	0.043	3.26	3.45	1452	1289	0.50	56.88	0.20	59	1.04	0.19	13.2	−8.2E−12	21	−8.7E−12	21	0.004	−26.1
KGA1B-ox-70.2.1	70	0.043	3.35	3.46	403	341	0.64	36.47	0.20	38	1.05	0.20	11.8	−5.5E−12	21	−5.9E−12	21	0.001	−23.2
KGA1B-ox-70.3.1	70	0.037	3.08	3.10	50	43	0.70	24.06	0.35	29	1.23	0.50	11.6	−1.2E−12	22	−1.4E−12	22	0.001	−18.2
KGA1B-ox-70.3.2	70	0.040	3.08	3.13	104	92	0.70	35.02	0.20	35	1.02	0.99	8.6	−2.0E−12	14	−2.0E−12	14	0.001	−19.9

nd, not determined.

[a] The first part of the name refers to the kaolinite sample that was used in the experiment, the digits following the letters ox are the experiment code, in which the first two digits refers to the temperature during the first stage of the experiment, and last digit marked the consecutive stage number of the experiment.

[b] Al/Si = Al/Si Stoichiometric ratio = $([Al_{output}] - [Al_{input}])/([Si_{output}] - [Si_{input}])$.

[c] Mass and area, mass or surface area of kaolinite.

[d] $Rate_{Al}$ and $Rate_{Si}$, kaolinite dissolution rate calculated using Eq. (4). Note that in our formalism, the rate is defined to be negative for dissolution.

[e] $\Delta Rate_{Al}$ and $\Delta Rate_{Si}$, the error (%) of the rate that was calculated using the Gaussian error propagation method (Eq. (5)).

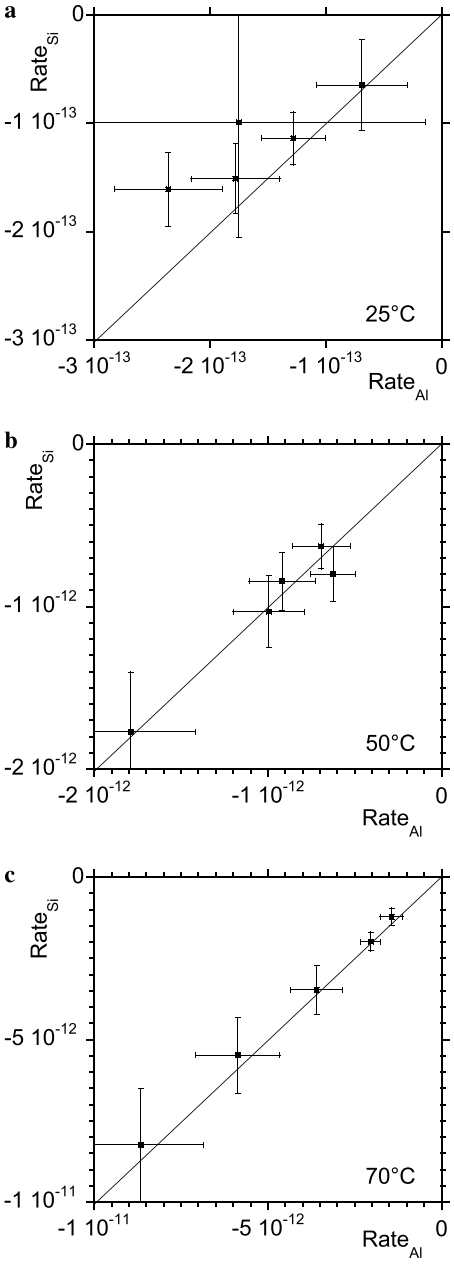

Fig. 2. Comparison of dissolution rates evaluated based on the total release of Al, $Rate_{Al}$, with those obtained based on the release of Si, $Rate_{Si}$ at (a) 25 °C, (b) 50 °C and (c) 70 °C. The solid lines are the 1/1 diagonal.

concentrations of the oxalate surface complexes (mol m^{-2}) were calculated using Eq. (7), and are shown in Table 3. We did not observe any significant differences between the adsorption on the surface of sample KGa-1 and KGa-1B nor between adsorption on surface of pretreated and untreated samples. The change of oxalate surface concentration on kaolinite as a function of the sum of oxalate and bioxalate activities in solution is shown in Fig. 4. Within the experimental variability, the oxalate adsorption at 25, 50, and 70 °C showed the same dependence on the sum of oxalate and bioxalate activities in solution (Fig. 4). The usage of this sum of activities is thoroughly discussed in Section 5.3.2.

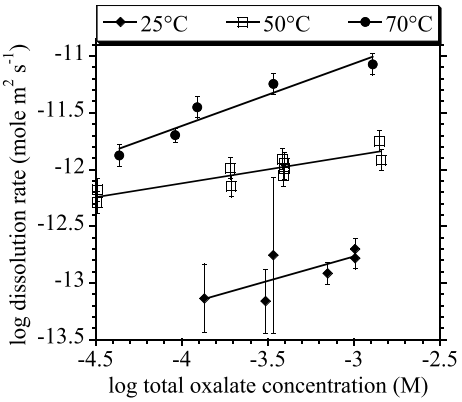

Fig. 3. The effect of oxalate concentration on the overall dissolution rate of kaolinite.

5. Discussion

5.1. The effect of oxalate on the overall dissolution rate of kaolinite

Fig. 3 plots the overall kaolinite dissolution rate as a function of the total concentration of oxalate. By plotting the log of the overall rate versus log of total oxalate concentration the data may be used to fit an empirical rate law of the form:

$$R_{TOT} = k_{ox} C_{ox}^{n}, \quad (9)$$

where k_{ox} is a rate coefficient, C_{ox} refers to the total concentration of oxalate in solution (M), and n is the reaction order with respect to oxalate concentration. The exponent n (which is represented by the slope of the lines in Fig. 3) is higher at 25 and 70 °C (0.45 and 0.55, respectively) than at 50 °C ($n = 0.24$). This empirical relation may be useful in reactive transport modeling in which experimental determined rate laws can be utilized. However, in order to understand the observed catalytic effect and to extrapolate the rate to other environmental conditions, the results should be examined using a rigorous mechanistic approach.

The observed enhancement of kaolinite dissolution rate by oxalate may be a result of direct or indirect effects of oxalate on the proton-promoted dissolution mechanism or a result of an alternative oxalate-promoted mechanism that affects the kaolinite, in addition to the proton-promoted mechanism. These two possible effects of oxalate on the overall dissolution rate of kaolinite are examined below.

5.2. Possible effects of oxalate on the proton-promoted dissolution rate

The rate of the proton-promoted dissolution of kaolinite is affected by the temperature, the pH, Al, and the degree of saturation. Cama et al. (2002) showed that under far from equilibrium conditions, the effects of pH and temperature on the overall dissolution rate of kaolinite under acidic conditions can be described by the equation:

Table 3
Experimental conditions and results of adsorption measurements

Experiment	Temperature (°C)	Kaolinite mass (g)	pH		[oxalate]		
			Initial	Final	Initial (μM)	Final (μM)	Surface (mol m^{-2})
iso-1400.1.0	25	1.006	2.74	2.92	1482	1068	5.1E−07
iso-2500.2.0	25	2.007	2.42	2.58	2699	1821	5.4E−07
iso-5000 pret	25	3.013	3.22	nd	5301	4199	4.4E−07
iso-7000 pret	25	3.023	3.22	nd	7190	6117	4.4E−07
iso-800.8	25	0.803	3.61	3.95	837	558	4.3E−07
iso-kga-1 B-pret-10	25	0.204	3.01	3.04	10	1	5.5E−08
iso-kga-1B-pret-100	25	0.403	3.09	3.14	104	30	2.3E−07
iso-kga-1B-pret-200	25	0.603	3.13	3.29	210	78	2.7E−07
iso-kga-1 B-pret-25	25	0.201	3.01	3.05	25	4	1.3E−07
iso-kga-1B-pret-400	25	0.809	3.24	3.49	407	216	2.9E−07
iso-kga-1B-pret-5	25	0.200	3.03	3.03	5	1	2.9E−08
iso-kga-1 B-pret-50	25	0.306	3.05	3.08	47	11	1.5E−07
kin-1400.8	25	0.805	2.80	2.87	1448	1126	5.0E−07
kin-400.6	25	0.603	3.24	3.48	420	253	3.4E−07
kin-400.8	25	0.808	3.24	3.53	420	209	3.2E−07
iso-ANT-10	25	0.207	3.11	3.24	10	4	3.6E−08
iso-ANT-100	25	0.404	3.15	3.34	117	49	2.1E−07
iso-ANT-1400	25	1.010	3.01	3.25	1525	1083	5.4E−07
iso-ANT-200	25	0.601	3.21	3.74	214	97	2.4E−07
iso-ANT-25	25	0.205	3.11	3.27	23	10	7.8E−08
iso-ANT-2500	25	1.536	2.97	3.28	2659	1965	5.6E−07
iso-ANT-400	25	0.803	3.33	4.37	413	229	2.9E−07
iso-ANT-5	25	0.202	3.13	3.24	6	2	2.8E−08
iso-ANT-50	25	0.303	3.12	3.30	38	18	8.2E−08
kin-50.6	25	0.809	3.22	3.31	52	12	6.1E−08
kin-50.8	25	0.809	3.22	3.35	52	8	6.7E−08
iso-5000.2 raw	25	2.008	2.83	3.14	5433	4593	5.0E−07
iso-kga-1 B-raw-10	25	0.202	3.01	3.04	10	1	5.4E−08
iso-kga-1 B-raw-100	25	0.403	3.09	3.13	104	39	1.9E−07
iso-kga-1B-raw-1400	25	1.008	2.71	2.78	1472	1080	4.7E−07
iso-kga-1 B-raw-200	25	0.602	3.13	3.22	210	103	2.1E−07
iso-kga-1 B-raw-25	25	0.202	3.01	3.04	25	6	1.1E−07
iso-kga-1 B-raw-400	25	0.800	3.24	3.46	407	247	2.4E−07
iso-kga-1B-raw-5	25	0.203	3.03	3.05	5.3	1.2	2.4E−08
iso-kga-1 B-raw-50	25	0.302	3.05	3.08	47	14	1.4E−07
iso-kga-1B-raw-800	25	1.001	3.57	3.87	846	508	4.1E−07
iso-50-5	50	0.201	nd	2.97	5.4	1.5	2.3E−08
iso-50-10	50	0.202	nd	2.98	10	3.2	3.9E−08
iso-50-25	50	0.205	nd	2.97	25	3.4	1.2E−07
iso-50-50	50	0.305	nd	2.98	49	10	1.5E−07
iso-50-100	50	0.400	nd	3.06	103	37	2.0E−07
iso-50-200	50	0.609	nd	3.33	205	95	2.2E−07
iso-50-400	50	0.808	nd	3.38	400	234	2.5E−07
iso-50-800	50	1.002	nd	4.23	768	511	3.1E−07
iso-50-1400	50	1.007	nd	3.05	1406	1042	4.3E−07
iso-50-2500	50	2.006	nd	3.14	2518	1795	4.3E−07
iso-50-4000	50	2.009	nd	2.99	3960	3084	5.2E−07
iso-50-5000	50	2.004	nd	3.35	5005	4156	5.1E−07
iso-50-7000	50	2.006	nd	3.26	6913	6073	5.0E−07
iso-50-2500/2.5	50	2.505	nd	3.59	2526	1764	3.7E−07
iso-50-4000/2.5	50	2.512	nd	3.38	4189	3197	4.8E−07
iso-50-800/0.7	50	0.706	3.00	3.11	849	617	4.0E−07
iso-50-1400/0.7	50	0.704	2.98	3.06	1469	1178	5.0E−07
iso-70-5	70	0.208	nd	3.03	5.3	1.7	2.1E−08
iso-70-10	70	0.207	nd	2.99	10	1.7	4.7E−08
iso-70-25	70	0.201	nd	3.05	24	1.5	1.4E−07
iso-70-50	70	0.306	nd	3.24	46	4.7	1.6E−07
iso-70-100	70	0.403	nd	3.24	98	22	2.3E−07
iso-70-200	70	0.605	nd	3.30	204	64	2.8E−07
iso-70-400	70	0.807	nd	3.60	391	196	2.9E−07
iso-70-1400	70	1.007	nd	3.26	1406	1038	4.4E−07
iso-70-2500/2.5	70	2.504	nd	4.00	2526	1784	3.6E−07
iso-70-4000/2.5	70	2.506	nd	3.74	4189	3283	4.4E−07

(*continued on next page*)

Table 3 (*continued*)

Experiment	Temperature (°C)	Kaolinite mass (g)	pH		[oxalate]		
			Initial	Final	Initial (μM)	Final (μM)	Surface (mol m^{-2})
iso-70-5000/2.5	70	2.506	nd	3.73	5073	4209	4.2E−07
iso-70-800/0.7	70	0.703	3.09	2.50	849	591	4.4E−07
iso-70-1400/0.7	70	0.702	3.06	3.18	1469	1188	4.8E−07

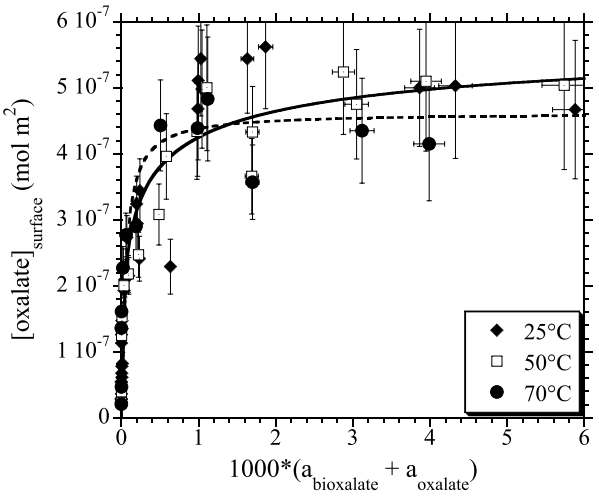

Fig. 4. Adsorption isotherms of oxalate on kaolinite in experiments that were conducted at pH 3, at 25, 50, and 70 °C. The surface concentration is plotted as a function of the sum of the activities of bioxalate and oxalate (see Section 5.3.2). The solid and the dashed lines are fitting of the general adsorption isotherm of Eq. (16) and the Langmuir adsorption isotherm, respectively, to all the experimental data.

$$\text{Rate} = 2\times10^{2}\cdot e^{-22/RT}\cdot\frac{2\times10^{-10}\cdot e^{19/RT}\cdot a_{H^+}}{1+2\times10^{-10}\cdot e^{19/RT}\cdot a_{H^+}} + 5\times10^{7}\cdot e^{-28/RT}\cdot\frac{1.4\times10^{-7}\cdot e^{10/RT}\cdot a_{H^+}}{1+1.4\times10^{-7}\cdot e^{10/RT}\cdot a_{H^+}}, \quad (10)$$

where R is the gas constant, T is the temperature (K), and a_{H^+} is the activity of protons in solution.

The ΔG_r of the kaolinite dissolution reaction is a strong function of the concentration of free aluminum in solution (Eq. (6)). As a result of the strong complexation of Al by oxalate, the solutions in the experiment with oxalate are more undersaturated than the solutions in experiments without oxalate. If the dissolution rate varied due to changes in ΔG_r in the different experiments, as the oxalate concentrations varied, then the oxalate effect would include an indirect effect on the proton-promoted mechanism. This indirect effect would be minimal only in the "far-from-equilibrium" dissolution plateau region, which is defined as the region in rate versus ΔG space where there is no direct effect of the degree of saturation on dissolution rate. As the dissolution rate of kaolinite is also directly affected by the pH and the aluminum activity, changes in pH and aluminum will cause both a direct effect and an indirect effect (via the degree of saturation) on dissolution rate. In contrast to aluminum, silicon does not have a direct effect on dissolution rate and thus does not affect the rate under far from equilibrium conditions (Devidal et al., 1997; Cama et al., 2002). Consequently, the direct effect of the degree of saturation on dissolution rate may be examined by manipulating the silicon concentration, as was done by Nagy et al. (1991). They showed that the dissolution plateau for kaolinite at 80 °C is reached for $\Delta G_r < -2$ kcal mol^{-1}, i.e., for ΔG_r below—2 kcal mol^{-1} kaolinite dissolution rate is not directly affected by the degree of under saturation. The results of Mogollon et al. (1996) show that the dissolution plateau for gibbsite at 25 °C is in very good agreement with the results of Nagy and Lasaga (1992) at 80 °C. Assuming that the dissolution plateau for kaolinite is similarly independent of temperature, our experimental range of ΔG_r, namely −18 to −29 kcal mol^{-1} (Table 2), is well within the dissolution plateau. Therefore, the observed oxalate effect on kaolinite dissolution rate (Fig. 3) did not result from the effect of the degree of saturation on the rate of the proton-promoted reaction mechanism.

Oelkers et al. (1994) and Devidal et al. (1997) showed a strong aluminum inhibition of kaolinite dissolution rate at 150 °C at saturated vapor pressure and pH 2. The Al inhibits the dissolution reaction even under very far from equilibrium conditions. Cama et al. (2002) showed that the effect of aluminum on kaolinite dissolution rate, at pH 3 and temperatures of 25, 50, and 70 °C, decreases with temperature. Whereas a significant inhibitory effect was observed at 50 °C and 70 °C (at pH 3), aluminum has little effect upon dissolution rate at 25 °C. Different mechanistic models were proposed in the literature for the inhibition of kaolinite dissolution rate at 150 °C by aluminum (Devidal et al., 1997; Ganor and Lasaga, 1998). All of these models may be adequately applied to the aluminum inhibition observed at 50 °C and 70 °C.

The activity of free aluminum (Al^{3+}) decreases significantly in the presence of oxalate due to the formation of Al-oxalate complexes (Table 4). Therefore, the proton-promoted dissolution rate in the presence of oxalate is expected to be significantly faster than that in an experiment with similar total Al concentration in the absence of oxalate. The major Al species in the experiments that were conducted in the presence of oxalate were $AlC_2O_4^+$ and $Al(C_2O_4)_2^-$. In most of these experiments the activity of free aluminum (Al^{3+}) was very low ($\leqslant 10^{-8}$ M, Table 4). In contrast, Al^{3+} is the dominant Al species in experiments that are conducted under acidic condition in the absence of oxalate, and therefore the total aluminum concentrations in experiments without oxalate are in the order of the concentrations of Al^{3+}. Using standard analytical techniques it is impossible to evaluate kaolinite dissolution rate when the total aluminum concentration is below 0.1 μM. Therefore,

Table 4
Calculated activities of species in solution and oxalate surface concentration in the flow-through experiments

Experiment[a]	a_{Al}[b]	a_{AlOx}[c]	a_{AlOx2}[d]	a_{AlOx3}[e]	aH_{Ox}[f]	a_{Ox}[g]	$a_{HOx} + a_{Ox}$	$Ox_{surface}$[h]
KGA1-ox-50.1.2	1.2E−10	4.4E−08	1.1E−06	6.3E−08	2.9E−04	3.0E−05	3.2E−04	3.5E−07
KGA1-ox-50.3.4	2.3E−10	8.5E−08	2.0E−06	1.2E−07	2.6E−04	2.9E−05	2.9E−04	3.4E−07
KGA1-ox-50.3.5	2.4E−09	2.7E−07	1.8E−06	3.2E−08	1.2E−04	8.7E−06	1.2E−04	2.8E−07
KGA1-ox-25.7.4	1.2E−09	5.2E−07	1.4E−05	1.0E−06	8.6E−04	3.5E−05	9.0E−04	4.2E−07
KGA1-ox-25.7.5-ANB	8.0E−10	3.9E−07	1.2E−05	9.3E−07	8.7E−04	3.9E−05	9.1E−04	4.2E−07
KGA1-ox-25.7.6	1.3E−09	4.1E−07	8.4E−06	4.3E−07	6.1E−04	2.6E−05	6.3E−04	4.0E−07
KGA1-ox-50.1.3	2.1E−10	9.7E−07	6.4E−06	1.1E−07	1.6E−04	8.3E−06	1.7E−04	3.0E−07
KGA1-ox-50.1.4	5.8E−09	2.8E−06	1.9E−06	3.3E−09	2.3E−05	8.6E−07	2.4E−05	1.7E−07
KGA1-ox-50.2.1	5.2E−11	6.5E−07	1.2E−05	5.2E−07	3.3E−04	2.2E−05	3.5E−04	3.6E−07
KGA1-ox-50.2.2	2.2E−10	1.1E−06	7.3E−06	1.2E−07	1.6E−04	8.6E−06	1.7E−04	3.0E−07
KGA1-ox-50.2.3	7.8E−09	4.0E−06	3.0E−06	5.4E−09	2.0E−05	9.2E−07	2.1E−05	1.6E−07
KGA1-ox-50.2.5	6.0E−11	7.3E−07	1.2E−05	5.2E−07	3.2E−04	2.1E−05	3.4E−04	3.5E−07
KGA1-ox-50.3.1	1.0E−10	1.3E−06	2.2E−05	9.9E−07	3.0E−04	2.2E−05	3.2E−04	3.5E−07
KGA1-ox-50.3.6	1.3E−10	1.9E−06	4.1E−05	2.2E−06	1.2E−03	2.7E−05	1.2E−03	4.4E−07
KGA1-ox-50.3B.7	1.9E−12	1.6E−07	1.9E−05	5.4E−06	1.1E−03	1.5E−04	1.3E−03	4.4E−07
KGA1B-ox-70.1.1	2.0E−10	7.2E−06	1.8E−05	1.1E−07	7.1E−05	3.1E−06	7.4E−05	2.4E−07
KGA1B-ox-70.1.2.2	7.6E−13	7.0E−07	4.4E−05	7.0E−06	1.0E−03	7.9E−05	1.1E−03	4.3E−07
KGA1B-ox-70.2.1	9.7E−12	2.2E−06	3.3E−05	1.3E−06	2.3E−04	1.9E−05	2.5E−04	3.3E−07
KGA1B-ox-70.3.1	6.8E−09	2.3E−05	5.2E−06	3.0E−09	8.1E−06	2.9E−07	8.4E−06	1.2E−07
KGA1B-ox-70.3.2	1.1E−09	1.6E−05	1.7E−05	4.6E−08	3.5E−05	1.3E−06	3.6E−05	2.0E−07

[a] See footnote in Table 1.
[b] a_{Al}, activity of Al^{+3}.
[c] a_{AlOx}, activity of $AlC_2O_4^+$.
[d] a_{AlOx2}, activity of $Al(C_2O_4)_2^-$.
[e] a_{AlOx3}, activity of $Al(C_2O_4)_3^{-3}$.
[f] a_{HOx}, activity of $HC_2O_4^-$.
[g] a_{Ox}, activity of $C_2O_4^{-2}$.
[h] $Ox_{surface}$, surface concentration of oxalate which was calculated using the general adsorption isotherm of Eq. (20).

it is impossible to directly determine the effect of Al on kaolinite dissolution rate at Al^{3+} concentrations that are similar to those in the experiment in the presence of oxalate.

Fig. 5 plots kaolinite dissolution rate as a function of the concentration of Al^{3+} in experiments conducted with and without oxalate at pH of about 3. In general, the dissolution rate in the presence of oxalate (with very low Al^{3+} concentrations) is much faster than in the absence of oxalate (and higher Al^{3+} concentrations). At 25 °C (Fig. 5a), Al inhibition is neither observed in the presence of oxalate nor in the absence of oxalate over a range of Al^{3+} concentration from 2 to 80 μM. A possible Al inhibition effect is observed at 50 and 70 °C both with and without oxalate (Figs. 5b and c). We argue that whereas the observed effect without oxalate is a real Al^{3+} inhibitory effect, the dissolution rate with oxalate is not affected by Al^{3+} inhibition due to the low concentration of Al^{3+}. The dissolution rates in experiments without oxalate and with Al^{3+} concentrations of few μM are within error the same as in the experiments conducted with relatively low concentrations of oxalate (few tens of μM), although in the latter the concentration of Al^{3+} was two to three orders of magnitude lower. For example, increasing the concentration of free Al^{3+} by 3 orders of magnitude, from 10^{-8} to 10^{-5} M, did not affect the dissolution rate (Fig. 5b). We suggest that a minimum concentration of a few tens of μM of free Al^{3+} is required to inhibit the dissolution rate of kaolinite, and therefore that reducing Al^{+3} further below 10 μM did not enhance kaolinite dissolution. Because the Al^{3+} concentrations in the experiments with oxalate are far below this apparent minimum inhibition concentration, the observed effect of oxalate likely does not reflect retardation of the direct aluminum inhibition due to the formation of Al-oxalate complexes.

The conclusion that the apparent effect of free Al^{3+} on kaolinite dissolution rate in the presence of oxalate (Fig. 5) is not related to Al inhibition is also supported by theoretical models. Several reaction mechanisms were proposed to explain the Al inhibition. In the present study, we will not repeat the theoretical background of the different mechanisms, which may be found in Oelkers et al. (1994), Oelkers and Schott (1998), and Ganor and Lasaga (1998), but merely present the resulting rate laws. Oelkers et al. (1994) proposed an Al inhibition model in which the dissolution rate of feldspar can be expressed by:

$$\text{Rate} = k_1 \cdot \left(\left(\frac{a_{H^+}^3}{a_{Al^{3+}}} \right)^n \Big/ \left(1 + K_1 \cdot \left(\frac{a_{H^+}^3}{a_{Al^{3+}}} \right)^n \right) \right), \tag{11}$$

where k_1 and K_1 are rate coefficient and equilibrium constant, respectively, n is a stoichiometric coefficient, and a_{H^+} and $a_{Al^{3+}}$ are the activity of H^+ and Al^{3+}, respectively. Ganor and Lasaga (1998) presented a mechanistic model describing the effects of an inhibitor on mineral dissolution

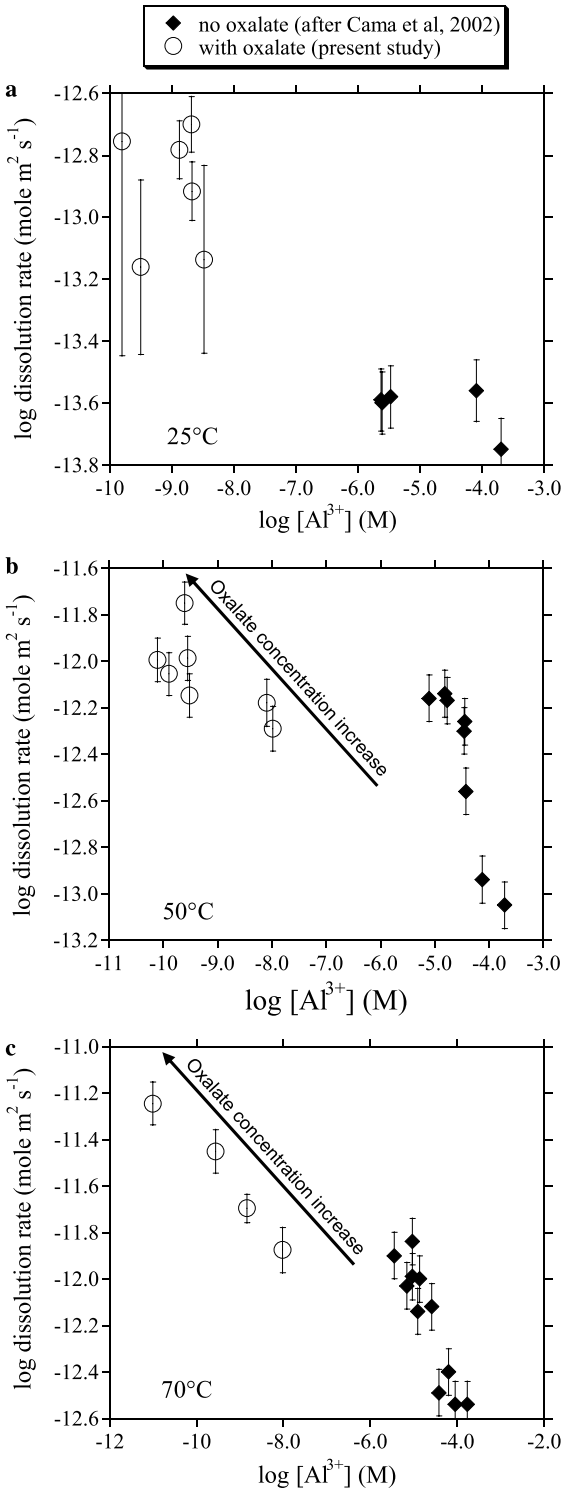

Fig. 5. Kaolinite dissolution rate as a function of the concentration of Al^{3+} in experiments conducted with and without oxalate at pH of about 3 and (a) 25 °C, (b) 50 °C, and (c) 70 °C.

rate in the presence of a catalyst. They proposed two end-member models: the competition model and the independent adsorption model. In the competition model, the catalyst and the inhibitor compete with each other. The rate law for this mechanism is:

$$\text{Rate} = k_2 \frac{b_{H^+} \cdot a_{H^+}}{1 + b_{H^+} \cdot a_{H^+} + b_{Al^{3+}} \cdot a_{Al^{3+}}}, \quad (12)$$

where k_2 is a rate coefficient and b_{H^+} and $b_{Al^{3+}}$ are adsorption constants. In the independent adsorption model proposed by Ganor and Lasaga (1998), the adsorption of the catalyst and the inhibitor are absolutely independent of each other. The rate law for this mechanism is:

$$\text{Rate} = k_3 \left(1 - k_4 \cdot \frac{b_{Al^{3+}} \cdot a_{Al^{3+}}}{1 + b_{Al^{3+}} \cdot a_{Al^{3+}}}\right) \cdot \frac{b_{H^+} \cdot a_{H^+}}{1 + b_{H^+} \cdot a_{H^+}}, \quad (13)$$

where k_3 and k_4 are rate coefficients. Figs. 6a–c plot log dissolution rate versus log activity of Al at constant pHs calculated from Eqs. (11)–(13), respectively. Fig. 6 shows that all the three models predict that the dissolution rate is independent of Al^{3+} for very low activity of Al^{3+}. Both the Al inhibition model of Oelkers et al. (1994) and the competition model predict that the rate would continue to decrease with increasing Al^{3+} until it approaches zero (or until the dissolution would be dominated by an alternative reaction mechanism), whereas according to the independent adsorption model, the dissolution rate is independent of Al^{3+} for both very low and very high activity of Al^{3+}. Neither of these models predicts the existence of an intermediate range of Al^{3+} in which dissolution rates would be independent of Al^{3+}, as is observed in Fig. 5. In other words, the prediction of the available models for Al inhibition indicates that the apparent effect of free Al^{3+} on kaolinite dissolution rate in the presence oxalate (Fig. 5) is not related to Al inhibition.

Our conclusion that the oxalate effect on kaolinite dissolution rate is not related to the effects of Al and deviation from equilibrium on the rate of the proton-promoted reaction mechanism corroborates the conclusion of Wieland and Stumm (1992) that oxalate catalyzes the kaolinite dissolution due to an oxalate-promoted mechanism, which affects the kaolinite in addition to the proton-promoted mechanism.

5.3. The oxalate-promoted dissolution mechanism

5.3.1. Calculating the rate of oxalate-promoted dissolution mechanism

At least two mechanisms should be considered when discussing kaolinite dissolution in the presence of oxalate under acidic conditions. The first is the oxalate-promoted (oxp) dissolution mechanism (Wieland and Stumm, 1992; Ganor and Lasaga, 1994). In this mechanism, an oxalate is adsorbed on the mineral surface, weakens the bonds, and as a result the mineral dissolution rate is enhanced. The second mechanism is the proton-promoted (pp) dissolution mechanism (Ganor et al., 1995; Huertas et al., 1999; Cama et al., 2002), in which proton adsorption on the mineral surface enhanced the dissolution of the mineral. Assuming that the two reaction paths occur independently (Furrer and Stumm, 1986), the overall dissolution rate is the sum of at least two terms:

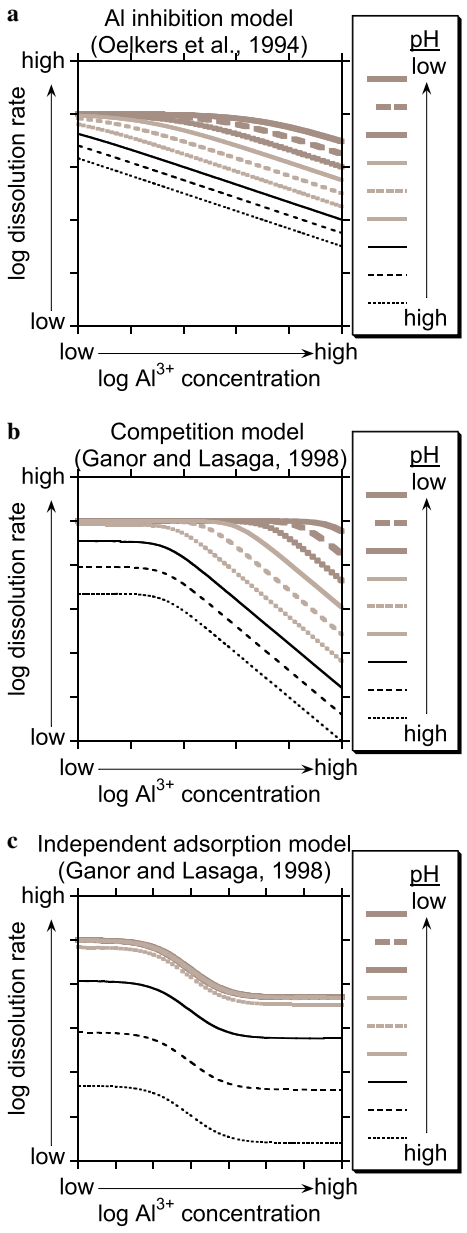

Fig. 6. Theoretical plots showing the effect of pH and Al^{3+} on dissolution rate as predicted by (a) the Al inhibition model of Oelkers et al. (1994), (b) the competition model, and (c) the independent adsorption model of Ganor and Lasaga (1998).

$$\text{Rate}_{\text{overall}} = \text{Rate}_{\text{pp}} + \text{Rate}_{\text{oxp}}. \tag{14}$$

The proton-promoted dissolution rate for each experiment was obtained based on the pH and the temperature using Eq. (10). The oxalate-promoted dissolution rate was calculated by subtracting the proton-promoted rate from the measured overall rate.

5.3.2. Surface speciation

A simple catalytic reaction mechanism consists of fast adsorption of the organic ion on the mineral surface followed by a rate-determining catalyst-mediated hydrolysis step. The rate of oxalate-promoted hydrolysis depends on the surface concentration of the ion. Therefore, the rate law must include the adsorption isotherms of the organic ion. The concentration of an ion (i) chemisorbed on the surface of a mineral may be described by a simple Langmuir adsorption isotherm:

$$C_{i,\text{s}} = F_i \frac{b_i \cdot a_i}{1 + b_i \cdot a_i}, \tag{15}$$

where $C_{i,\text{s}}$ is the surface concentration of i (mol m^{-2}), F_i is the maximum surface coverage of i (mol m^{-2}), b_i is an adsorption constant, and a_i is the activity of i in the solution. By substituting a Gaussian adsorption energy distribution function into the Langmuir model one obtains an integrated adsorption isotherm of the non-linear form (Adamson, 1990):

$$C_{i,\text{s}} = F_i \frac{b_i \cdot a_i^{n_i}}{1 + b_i \cdot a_i^{n_i}}, \tag{16}$$

where n_i is a coefficient. This non-linear adsorption isotherm reduces to the Freundlich empirical adsorption isotherm at low concentration of i:

$$C_{i,\text{s}} = K_i \cdot a_i^{n_i}, \tag{17}$$

where K_i is an adsorption coefficient (mol m^{-2}). Both the Freundlich and the Langmuir isotherms are special cases of the general model of Eq. (16).

The general adsorption isotherm of Eq. (16) relates the surface concentration of i to its activity in solution and ignores the possibility that more than one type of ion may be adsorbed onto the same surface site. For the case of adsorption of m different ions on the same surface site, one should use a multi-term adsorption isotherm such as:

$$C_{\text{tot,s}} = F_{\text{tot}} \frac{\sum_{i=1}^{m} (b_i \cdot a_i^{n_i})}{1 + \sum_{i=1}^{m} (b_i \cdot a_i^{n_i})}, \tag{18}$$

where $C_{\text{tot,s}}$ is the sum of the surface concentrations of the different ions (mol m^{-2}) and F_{tot} is the maximum surface coverage of these elements (mol m^{-2}). Using this approach with a Langmuir adsorption isotherm (i.e., $n_i = 1$), Stillings et al. (1998) fitted the total adsorption of oxalate on andesine surface and obtained the equation:

$$C_{\text{s,ox}} = 2.48 \times 10^{-6} \cdot \frac{1120 \cdot a_{HC_2O_4^-} + 1966 \cdot a_{C_2O_4^{2-}}}{1 + 1120 \cdot a_{HC_2O_4^-} + 1966 \cdot a_{C_2O_4^{2-}}}. \tag{19}$$

The resulting equilibrium constant for the adsorption of oxalate is 40% larger than that for bioxalate. It is important to note that as in many other surface complexation models (e.g., Ganor et al., 2003), the resulting coefficients are not well constrained. Therefore, different combinations of the two equilibrium constants for the adsorption of bioxalate and oxalate yield similar curves that adequately describe the experimental data. For example, if we fit the andesine data of Stillings et al. (1998) using the same equilibrium constant for oxalate and bioxalate, the resulting regression coefficient ($R^2 = 0.952$) is similar to the regression coefficient obtained using Eq. (19) ($R^2 = 0.957$).

Following the approach of Stillings et al. (1998), we fitted a two-term Langmuir adsorption isotherm to the total adsorption of oxalate on kaolinite surface using the activities of oxalate and bioxalate as the independent variables. For the 25 °C data, the best fit curve was obtained for $F_{tot} = 5.6 \times 10^{-7}$, $b_{HC_2O_4^-} = 9982$ and $b_{C_2O_4} = 0$, and the regression coefficient $R^2 = 0.92$. Similarly, for 50 and 70 °C the best fit curves were obtained when the equilibrium constant for oxalate adsorption, $b_{C_2O_4}$, was zero.

The speciation of oxalate in solution depends both on the pH and on the concentration of aluminum. At pH of about 3 and in the absence of aluminum almost all of the oxalate in solution is negatively charged as bioxalate (93–95%) and oxalate (2.7–5%). The adsorption experiments in the present study were conducted under a limited range of $2.5 < pH < 3.5$. As a result there is a very strong linear correlation between the activity of oxalate and bioxalate ($R^2 = 0.8$). Due to this linear correlation other combinations of the two equilibrium constants for the adsorption of bioxalate and oxalate yield similar curves that adequately describe the experimental data. For example, if one fits Eq. (15) to the 25 °C data using the oxalate activity as the independent variable, the obtained regression coefficient is reasonably good ($R^2 = 0.84$). Therefore, the adsorption data in the present study cannot be used to estimate the relative importance of the adsorption of oxalate and bioxalate. Fitting a two-term general adsorption isotherm instead of a two-term Langmuir adsorption isotherm did not improve our ability to estimate the relative importance of the adsorption of oxalate and bioxalate.

Axe and Persson (2001), Yoon et al. (2004), and Persson and Axe (2005) used Attenuated Total Reflectance Fourier Transform Infrared (ATR-FTIR) Spectroscopy to study the types and structures of adsorption complexes of oxalate at mineral/water interfaces of boehmite, corundum and goethite. They identified both inner-sphere (i.e., a complex with a direct bond between the carboxylate group and the surface metal ion) and outer-sphere (i.e., no direct bond between the carboxylate group and the surface metal ion) complexes. Yoon et al. (2004) compared the adsorption of oxalate on boehmite at pH 2.5, where bioxalate is the dominant species in aqueous solution to that at pH 5.1, where oxalate is the dominant species. Regardless of the differences in oxalate speciation in solution, similar adsorbed oxalate spectral features were measured at pH 2.5 and 5.1. This observation suggests that the coordination geometries of adsorbed oxalate and adsorbed bioxalate species are either the same or very similar. As for the adsorption data, the ATR-FTIR data cannot be used to estimate the relative importance of the adsorption of oxalate and bioxalate. Therefore, we modeled and plotted the total surface concentration of oxalate as a function of the sum of the activities of bioxalate and oxalate (Fig. 4). Within the experimental variability, the oxalate adsorption at 25, 50, and 70 °C showed the same dependence on the sum of oxalate and bioxalate activities in solution. Therefore, we fitted the general adsorption isotherm of Eq. (16) using the entire data set at 25, 50, and 70 °C. This fitting (solid line in Fig. 4) yields the isotherm:

$$C_{s,ox} = 6.1 \times 10^{-7} \cdot \frac{64 \cdot \left(a_{HC_2O_4^-} + a_{C_2O_4^{2-}}\right)^{0.48}}{1 + 64 \cdot \left(a_{HC_2O_4^-} + a_{C_2O_4^{2-}}\right)^{0.48}}, \quad (20)$$

where $C_{s,ox}$ is the total concentration of oxalate on the kaolinite surface (mol m^{-2}) and $a_{HC_2O_4^-}$ and $a_{C_2O_4^{2-}}$ are the activities of bioxalate and oxalate, respectively. Fitting the Langmuir adsorption isotherm (dashed line in Fig. 4) to the same data set yields the isotherm:

$$C_{s,ox} = 4.6 \times 10^{-7} \cdot \frac{18,333 \cdot \left(a_{HC_2O_4^-} + a_{C_2O_4^{2-}}\right)}{1 + 18,333 \cdot \left(a_{HC_2O_4^-} + a_{C_2O_4^{2-}}\right)}. \quad (21)$$

The regression coefficient for the fitting of the Langmuir adsorption isotherm ($R^2 = 0.85$) is somewhat lower than that for the fitting of the general adsorption isotherm ($R^2 = 0.90$). This is expected as the Langmuir isotherm is a special case of the general adsorption isotherm. Taking into account the experimental variability, both Eqs. (20) and (21) adequately describe the experimental data. In the following discussion, we will use the general adsorption isotherm (Eq. (20)) to predict the surface concentration of oxalate in the dissolution experiments. Predicting the surface concentration using the Langmuir adsorption isotherm would not affect any of our conclusions regarding the oxalate-promoted dissolution mechanism.

5.3.3. The traditional oxalate-promoted dissolution mechanism

The discussion of the oxalate-promoted dissolution mechanism is based on the following assumptions: (1) the oxalate-promoted reaction mechanism is independent of the proton-promoted mechanism; (2) oxalate-promoted reaction mechanism consists of fast adsorption of oxalate species on a kaolinite surface site(s) followed by a slow hydrolysis step; (3) the adsorption of the oxalate species on the kaolinite surface may be described by the general adsorption isotherm of Eq. (20); and (4) the different adsorbed oxalate species formed similar surface complexes (Yoon et al., 2004), and therefore have the same effect on the bond strength and hence on dissolution rate. If steady-state conditions are maintained, the rate of the oxalate-promoted reaction mechanism ($Rate_{oxp}$, mol m^{-2} s^{-1}) is (Lasaga, 1981):

$$Rate_{oxp} = k_1 \cdot C_{s,ox}, \quad (22)$$

where k (s^{-1}) is the rate coefficient of the oxalate-promoted reaction mechanism. The speciation of oxalate in solution for each of the dissolution experiments is presented in Table 4. Based on these data, the surface concentration of oxalate was calculated using Eq. (20). Fig. 7 plots the dependence of the oxalate-promoted dissolution rate at each temperature on the calculated oxalate surface concentration. As predicted by Eq. (22), the observation may be

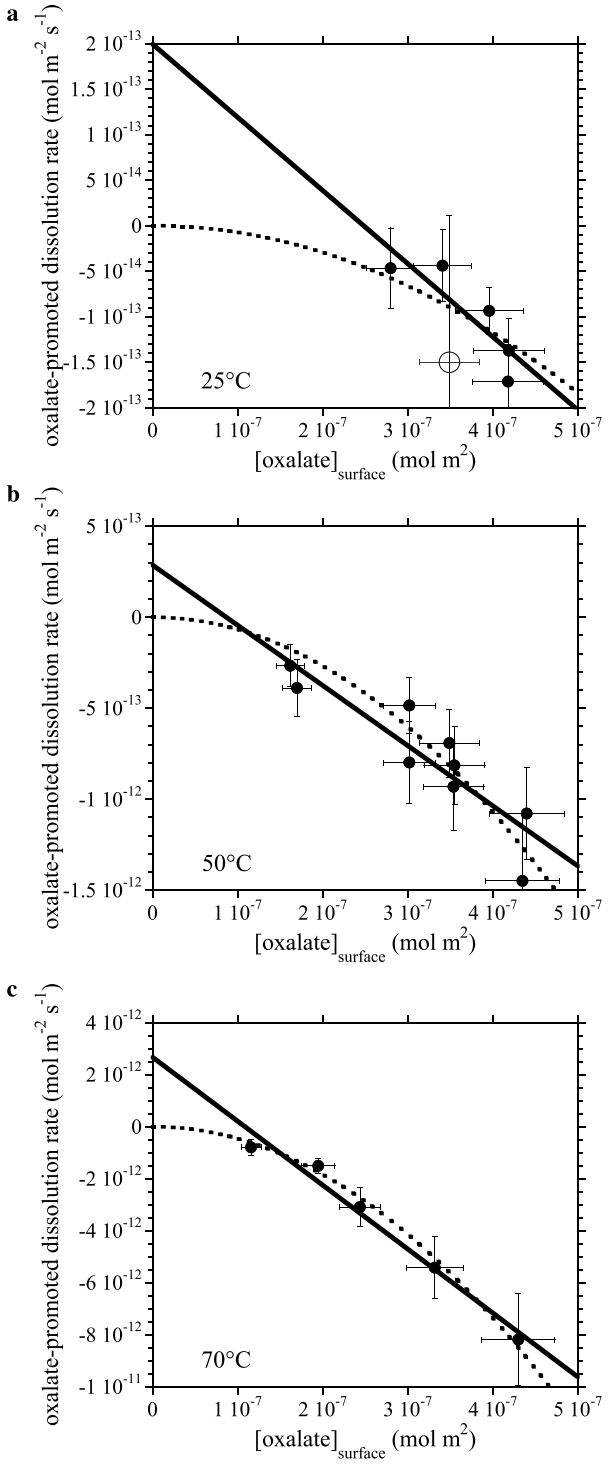

Fig. 7. The dependence of the rate of the oxalate-promoted dissolution mechanism on the total surface concentration of oxalate at (a) 25 °C, (b) 50 °C, and (c) 70 °C. The solid lines are fitting of the data to the traditional oxalate-promoted reaction mechanism of Eq. (22). The dashed lines are the fitting of the experimental data to the quadratic rate law of Eq. (23). The data point in (a) which is marked by an open symbol was not included in the regression calculations, due to its high uncertainty.

adequately described using a linear regression (solid lines in Fig. 7). The obtained slopes (k in Eq. (22)) are $8 \pm 3 \times 10^{-7}$, $3.3 \pm 0.6 \times 10^{-6}$, and $2.5 \pm 0.3 \times 10^{-5}$ s^{-1} at 25, 50, and 70 °C, respectively. In contrast to the prediction of Eq. (22), the regression lines in Fig. 7 do not cross through the origin, and the oxalate-promoted rate becomes 0 when the oxalate surface concentrations are in the range of 0.1–0.2 μmol m^{-2} (i.e., when the sum of the activities of oxalate and bioxalate in solution is in the range of 5–40×10^{-6}). The conclusion, that there is a threshold of oxalate concentration that is required to catalyze the kaolinite dissolution, is in accordance with the general observation that the effect of oxalate on silicate dissolution becomes significant at total oxalate concentration of around 1 mM (Drever and Stillings, 1997). A possible explanation for this observation is that oxalate initially adsorbed on surface sites in which it forms surface complexes that do not affect the bond strength. Only after filling these surface sites, oxalate starts to form surface complexes that weaken the bond strength, and therefore catalyzes the kaolinite dissolution. To examine this possibility, the possible adsorption sites on kaolinite are detailed below.

Taking into account the strong complexation between Al and oxalate in solution, it seems reasonable that the adsorption of oxalate would occur initially on aluminol sites rather than on silanol sites. In theory, oxalate may adsorb both on the edge and the basal plain of the kaolinite. Yet, it was widely recognized in recent studies that dissolution and precipitation of phyllosilicates occur preferentially at the edge, i.e., the (*hk0*) surfaces (e.g., Novak and Cicel, 1978; Luca and MacLachlan, 1992; Kaviratna and Pinnavaia, 1994; Turpault and Trotignon, 1994; Kalinowski and Schweda, 1996; Bickmore et al., 1999; Rufe and Hochella, 1999; Bosbach et al., 2000). Although basal plane dissolution may contribute to some extent to phyllosilicate bulk dissolution rate (Blum, 1994; Huertas et al., 1999; Cama et al., 2002; Brandt et al., 2003; Ganor et al., 2003), the dissolution process is dominated by the chemical attack on edge sites. Therefore, it could be suggested that oxalate initially adsorbs on specific sites on the basal plane (e.g., defects). Only after filling these sites, oxalate would start to catalyze dissolution by forming oxalate complexes on the edge aluminol sites. Although we cannot reject this explanation, the possibility that oxalate would initially adsorb to the basal plane rather than to the edges seems improbable. In any case, the results of the present study do not provide any independent evidence that may support the suggestion that oxalate initially adsorbed to the basal planes.

Alternatively, one can suggest that oxalate initially formed outer-sphere complexes on the kaolinite surface, which do not catalyze the kaolinite dissolution. Currently, there are no published data on the complexation of oxalate on kaolinite surface. ATR-FTIR studies of boehmite, corundum, and goethite (Axe and Persson, 2001; Yoon et al., 2004; Persson and Axe, 2005) reveal that the dominant oxalate-surface complexes at low concentration of oxalate are inner-sphere complexes, which are presumably responsible for the enhancement of the dissolution rate (Stumm, 1992). If this is the case for adsorption of oxalate

on kaolinite surface, the above explanations for the threshold of oxalate concentration that is required to catalyze the kaolinite dissolution do not hold, and an alternative oxalate-promoted reaction mechanism should be examined.

5.3.4. The proposed rate law for the oxalate-promoted dissolution of kaolinite

One of the important assumptions of the traditional oxalate-promoted reaction mechanism is that the effect of each surface oxalate complex on dissolution is the same, and that this effect is not influenced by the presence or absence of the other oxalate complexes. If this assumption does not hold, the rate is not linearly proportional to the oxalate concentration on the surface. Indeed, the observations in Fig. 7 are better described using a quadratic rate law of the form:

$$\mathrm{Rate}_{\mathrm{oxp}} = k_2 \cdot C_{\mathrm{s,ox}}^2, \tag{23}$$

where k_2 ($\mathrm{m^2\ mol^{-1}\ s^{-1}}$) is the rate coefficient for the quadratic rate law. The quadratic rate law of Eq. (23) was fitted to the calculated oxalate-promoted rates at each temperature using non-linear regression (dashed lines in Fig. 7). The obtained k_2 values are 0.7 ± 0.1, 6.7 ± 0.4, and $46 \pm 1\ \mathrm{m^2\ mol^{-1}\ s^{-1}}$ at 25, 50, and 70 °C, respectively. Theoretically, a quadratic rate law may be justified if the reaction is catalyzed by the simultaneous adsorption of two ligands on or near the same surface site.

Based on crystallographic considerations, Sposito (1984) estimated the density of aluminol sites on kaolinite edges to be 1 site per $0.379\ \mathrm{nm^{-2}}$ of edge surface area. In order to determine the surface density of the aluminol on the edge per total surface area, this figure should be multiplied by the percentage of the edge surface area. Sposito (1984) estimated that the edge surface area of kaolinite is 7.9% of the total surface area, resulting in a total edge aluminol surface density of ≈0.2 sites $\mathrm{nm^{-2}}$ or $3.46 \times 10^{-7}\ \mathrm{mol\ m^{-2}}$. For relatively high activities of oxalate + bioxalate in solution ($>1 \times 10^{-3}$) the average surface concentration of oxalate is $4.8 \pm 0.5 \times 10^{-7}\ \mathrm{mol\ m^{-2}}$. This value, which is within error equal to the maximum surface coverage of oxalate that is predicted from the fitting of the Langmuir adsorption isotherm ($4.6 \times 10^{-7}\ \mathrm{mol\ m^{-2}}$, Eq. (21)), is larger than the estimated amount of available edge aluminol sites by 38%. Based on Scanning Force Microscopy measurements, Brady et al. (1996) showed that percentage of kaolinite edge surface area from the total surface area may be significantly larger than the estimation of 7.9% of Sposito (1984). Therefore, the observation that the amount of adsorbed oxalate is somewhat larger than the estimated amount of available edge aluminol does not prove that oxalate adsorbed on other sites.

In the present study, we found that increasing the activities of oxalate + bioxalate from 1×10^{-3} to 6×10^{-3} does not cause any significant increase in the surface concentration of oxalate (Fig. 4). This last observation indicates that the kaolinite surface becomes saturated with respect to oxalate at surface concentration of about $5 \times 10^{-7}\ \mathrm{mol\ m^{-2}}$ (0.3 sites $\mathrm{nm^{-2}}$). This value is significantly smaller than the estimated site density on kaolinite basal surface planes (≈4 sites $\mathrm{nm^{-2}}$). The simple explanation for the similarity between the saturation density of oxalate on the kaolinite surface and edge aluminol surface density is that oxalate adsorption occurs mainly on the edges rather than on the basal planes. If indeed the adsorption of oxalate occurs mainly on kaolinite edges, which are close to be fully occupied by oxalate, than in many of these sites two oxalate complexes must be formed on neighboring surface sites, if not on the same site. The ATR-FTIR data of Axe and Persson (2001), Yoon et al. (2004), and Persson and Axe (2005) did not reveal the existence of a surface complex that is composed of two oxalates that are attached to the same metal site. Therefore, it is more likely that the quadratic rate law represents catalysis by the adsorption of two oxalates on two neighboring metal sites. As we do not have any direct evidence that the proposed oxalate-promoted dissolution mechanism is indeed the catalytic reaction mechanism, one can view the quadratic rate law of Eq. (23) as an empirical rate law.

5.4. The effect of temperature on the oxalate-promoted rate

The temperature dependence of dissolution rate generally follows the Arrhenius law:

$$\mathrm{Rate} = A\,\mathrm{e}^{-E_a/RT}, \tag{24}$$

where A ($\mathrm{mol\ m^{-2}\ s^{-1}}$) is the pre-exponential factor, E_a ($\mathrm{cal\ mol^{-1}}$) is the apparent activation energy, R ($\mathrm{cal\ mol^{-1}\ K^{-1}}$) is the gas constant, and T is the temperature (K). Fig. 8 plots the natural log of the rate coefficient k_2, at 25, 50, and 70 °C versus $1/T$. Apparent activation energy of $18{,}600 \pm 1200\ \mathrm{cal\ mol^{-1}}$ and a pre-exponential factor of $3 \pm 5 \times 10^{13}\ \mathrm{mol\ m^{-2}\ s^{-1}}$ were calculated using Eq. (24) from a least squares estimate of the slope of the plot. Using the quadratic rate law, the oxalate-promoted dissolution rate of kaolinite at pH 3 and temperature from 25 to 70 °C may be predicted using the equation:

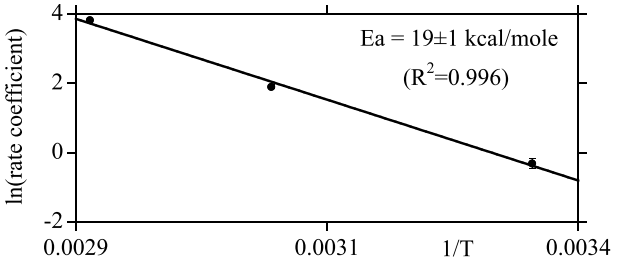

Fig. 8. Arrhenius plot of the rate coefficients k_2 of the quadratic rate law, which was obtained from the fitting of the experimental data to Eq. (23).

$$\begin{aligned}\mathrm{Rate}_{\mathrm{oxp}} &= 3\cdot 10^{13}\,\mathrm{e}^{-18{,}600/1.987T}\cdot C_{\mathrm{s,ox}}^{2}\\ &= 3\cdot 10^{13}\,\mathrm{e}^{-18{,}600/1.987T}\\ &\quad\cdot\left(6.1\times 10^{-7}\cdot\frac{64\cdot\left(a_{HC_2O_4^-}+a_{C_2O_4^{2-}}\right)^{0.48}}{1+64\cdot\left(a_{HC_2O_4^-}+a_{C_2O_4^{2-}}\right)^{0.48}}\right)^{2}.\end{aligned}\tag{25}$$

6. Summary and conclusions

The effect of oxalate on kaolinite dissolution rates was examined using non-mixed flow-through reactors at 25, 50, and 70 °C in a pH of about 3 under far-from equilibrium conditions ($-29 < \Delta G_r < -18$ kcal mol^{-1}). It was found that kaolinite dissolution rate was catalyzed by oxalate. The observed enhancement of kaolinite dissolution rate is the result of an oxalate-promoted mechanism that affects the kaolinite in addition to the proton-promoted mechanism, and not the result of effects of oxalate on the proton-promoted dissolution mechanism. This observation is in accordance with the conclusion of Wieland and Stumm (1992). We suggest that the observation that adsorption of oxalate on kaolinite surface catalyzed the kaolinite dissolution supports the conclusion of Stillings et al. (1998) that oxalate surface complexation catalyzes andesine dissolution and challenges the suggestion of Oelkers and Schott (1998) that organic anion surface adsorption has a negligible effect on alkali-feldspar dissolution rates. We do not suggest that the surface reaction is identical for the two minerals, as the Al is octahedrally coordinated in the kaolinite structure and is tetrahedrally coordinated in the feldspar structure. It is important to note that in order to be able to prove that kaolinite is affected by the oxalate-promoted mechanism, the experiments of the present study were conducted under conditions in which the effects of oxalate on the proton-promoted mechanism are negligible (i.e., with Al free input solution at pH near 3, and far-from-equilibrium). Therefore, we do not argue that the proton-promoted mechanism is not influenced by the presence of oxalate under different experimental conditions.

The oxalate-promoted dissolution rate shows a linear dependence on the calculated sum of activities of oxalate and bioxalate on the surface, as is predicted by the traditional oxalate-promoted reaction mechanism. However, for lower surface concentrations (<0.2 μmol m^{-2}), the catalytic effect of oxalate is significantly smaller than is predicted by the linear trend. A better fit is obtained if one uses a quadratic rate law, i.e., a rate law in which the oxalate-promoted dissolution rate depends on the square of the oxalate surface concentration. We propose two alternative explanations for the observations of the present study: (1) oxalate initially adsorbs on surface sites at which it forms surface complexes that do not affect the rate of kaolinite dissolution; and (2) the dissolution is catalyzed by the simultaneous adsorption of two ligands on or near the same surface site. We cannot definitively rule out any of these alternative interpretations. However, taking into account the structure and the available adsorption sites on the kaolinite surface, the first explanation seems unreasonable to us. Spectroscopic studies of oxalate complexes at oxides/water interfaces do not reveal any evidence that two oxalates may form a complex with a single Al on the surface. Therefore, we suggest that the bond strength is significantly weakened only when Al-oxalate complexes are formed on two neighboring edge aluminol sites. The present study shows that at adsorptive saturation, the amount of adsorbed oxalate is comparable to the amount of available kaolinite Al edge sites, and is much smaller than the amount of available Al surface sites on the basal planes. This is consistent with the adsorption of oxalate mainly on edge aluminol sites, and with the idea that the formation of Al-oxalate complexes on two neighboring edge aluminol sites must be common, above a threshold oxalate concentration.

Our proposed mechanism shows a good agreement with the observed effect of oxalate on kaolinite dissolution and its predictions are significantly better than those of the traditional oxalate-promoted reaction mechanism. Further spectroscopic and theoretical calculations are required to confirm or refute the above proposal.

Acknowledgments

This research was supported by Grant # 94-00089 from the United States-Israel Binational Science Foundation and by a seed money grant from the Research and Development Authority at Ben-Gurion University of the Negev. We thank Lisa Stillings and two anonymous reviewers for their thorough reviews that significantly improved the quality of the manuscript. The handlings of the manuscript by the associate editor, Carrick Eggleston, as well as his comments are gratefully acknowledged. Ellen Faller from the Yale Peabody Museum and John Yang from the Clay Mineral Society kindly supplied the kaolinite samples. We wish to express our gratitude to A. C. Lasaga, A. Sivan, and V. Metz for fruitful discussions and to E. Shani, A. Avital, E. Roueff, G. Ronen, O. Halabi, and V. Pavlov for their technical assistance.

Associate editor: Carrick M. Eggleston

References

Adamson, A.W., 1990. *Physical Chemistry of Surfaces*. Wiley, Chichester.

Amram, K., Ganor, J., 2005. The combined effect of pH and temperature on smectite dissolution rate under acidic conditions. *Geochim. Cosmochim. Acta* **69** (10), 2535–2546.

Axe, K., Persson, P., 2001. Time-dependent surface speciation of oxalate at the water-boehmite (γ-AlOOH) interface: Implications for dissolution. *Geochim. Cosmochim. Acta* **65** (24), 4481–4492.

Barrante, J.R., 1974. *Applied Mathematics for Physical Chemistry*. Prentice-Hall, Englewood Cliffs, NJ.

Bell, J.L.S., Palmer, D.A., 1994. Experimental studies of organic acid decomposition. In: Pittman, E.D., Lewan, M.D. (Eds.), *Organic Acids in Geological Processes*. Springer-Verlag, Berlin, pp. 226–269.

Bell, J.L.S., Palmer, D.A., Barnes, H.L., Drummond, S.E., 1994. Thermal decarboxylation of acetate: III. Catalysis by mineral surfaces. *Geochim. Cosmochim. Acta* **58** (19), 4155–4177.

Bennett, P.C., Casey, W., 1994. Chemistry and mechanisms of low-temperature dissolution of silicates by organic acids. In: Pittman, E.D., Lewan, M.D. (Eds.), *Organic Acids in Geological Processes*. Springer-Verlag, Berlin, pp. 162–200.

Bickmore, B.R., Hochella, M.F.J., Bosbach, D., Charlet, L., 1999. Methods for performing atomic force microscopy imaging of clay minerals in aqueous solution. *Clay Clay Miner.* **47**, 573–581.

Blake, R.E., Walter, L.M., 1996. Effects of organic acids on the dissolution of orthoclase at 80 °C and pH 6. *Chem. Geol.* **132**, 91–102.

Blake, R.E., Walter, L.M., 1999. Kinetics of feldspar and quartz dissolution at 70–80 °C and near-neutral pH: effects of organic acids and NaCl. *Geochim. Cosmochim. Acta* **63** (13-14), 2043–2059.

Blum, A.E., 1994. Determination of illite/smectite particle morphology using scanning force microscopy. In: Nagy, K.L., Blum, A.E. (Eds.), *Scanning Probe Microscopy of Clay Minerals*. Clay Minerals Society, pp. 172–203.

Bosbach, D., Charlet, L., Bickmore, B.R., Hochella, M.F.J., 2000. The dissolution of hectorite: in-situ, real-time observations using Atomic Force Microscopy. *Am. Mineral.* **85**, 1209–1216.

Brady, P.V., Cygan, R.T., Nagy, K.L., 1996. Molecular control on kaolinite surface charge. *J. Colloid Interface Sci.* **183**, 356–364.

Brandt, F., Bosbach, D., Krawczyk-Barsch, E., Arnold, T., Bernhard, G., 2003. Chlorite dissolution in the acid pH-range: a combined microscopic and macroscopic approach. *Geochim. Cosmochim. Acta* **67** (8), 1451–1461.

Busey, R.H., Mesmer, R.E., 1978. Thermodynamic quantities for the ionization of water in sodium chloride media to 300 °C. *J. Chem. Eng. Data* **23**, 175–176.

Cama, J., Metz, V., Ganor, J., 2002. The effect of pH and temperature on kaolinite dissolution rate under acidic conditions. *Geochim. Cosmochim. Acta* **66** (22), 3913–3926.

Carroll, S.A., Walther, J.V., 1990. Kaolinite dissolution at 25°, 60°, and 80 °C. *Am. J. Sci.* **290**, 797–810.

Carroll-Webb, S.A., Walther, J.V., 1988. A surface complex reaction model for the pH-dependence of corundum and kaolinite dissolution rates. *Geochim. Cosmochim. Acta* **52**, 2609–2623.

Chin, P.-K.F., Mills, G.L., 1991. Kinetics and mechanisms of kaolinite dissolution: effects of organic ligands. *Chem. Geol.* **90**, 307–317.

Crossey, L.J., 1991. Thermal degradation of aqueous oxalate species. *Geochim. Cosmochim. Acta* **55**, 1515–1527.

Devidal, J.-L., Schott, J., Dandurand, J.-L., 1997. An experimental study of kaolinite dissolution and precipitation kinetics as a function of chemical affinity and solution composition at 150 °C, 40 bars, and pH 2, 6.8, and 7.8. *Geochim. Cosmochim. Acta* **61** (24), 5165–5186.

Drever, J.I., Stillings, L.L., 1997. The role of organic acids in mineral weathering. *Colloids Surfaces A* **120**, 167–181.

Drever, J.I., Vance, G.F., 1994. Role of soil organic acids in mineral weathering processes. In: Pittman, E.D., Lewan, M.D. (Eds.), *Organic Acids in Geological Processes*. Springer-Verlag, Berlin, pp. 138–161.

Fox, T.R., Comerford, N.B., 1990. Low-molecular-weight organic acids in selected soils of the southeastern USA. *Soil Sci. Soc. Am. J.* **54**, 1139–1144.

Franklin, S.P., Hajash, A.J., Dewers, T.A., Tieh, T.T., 1994. The role of carboxylic acids in albite and quartz dissolution: an experimental study under diagenetic conditions. *Geochim. Cosmochim. Acta* **58** (20), 4259–4279.

Furrer, G., Stumm, W., 1986. The coordination chemistry of weathering: I. Dissolution kinetics of Δ-Al_2O_3 and BeO. *Geochim. Cosmochim. Acta* **50**, 1847–1860.

Ganor, J., Cama, J., Metz, V., 2003. Surface protonation data of kaolinite—reevaluation based on dissolution experiments. *J. Colloid Interface Sci.* **264**, 67–75.

Ganor, J., Lasaga, A.C., 1994. The effects of oxalic acid on kaolinite dissolution rate. *Mineral. Mag.* **58A**, 315–316.

Ganor, J., Lasaga, A.C., 1998. Simple mechanistic models for inhibition of a dissolution reaction. *Geochim. Cosmochim. Acta* **62** (8), 1295–1306.

Ganor, J., Metz, V., 2001. To stir or not to stir—implications for silicate dissolution experiments. In: *10th International Symposium on Water–Rock Interaction*, pp. 271–274.

Ganor, J., Mogollon, J.L., Lasaga, A.C., 1995. The effect of pH on kaolinite dissolution rates and on activation energy. *Geochim. Cosmochim. Acta* **59**, 1037–1052.

Ganor, J., Mogollon, J.L., Lasaga, A.C., 1999. Kinetics of gibbsite dissolution under low ionic strength conditions. *Geochim. Cosmochim. Acta* **63** (11–12), 1635–1651.

Ganor, J., Nir, S., Cama, J., 2001. The effect of kaolinite on oxalate (bio)degradation at 25 °C, and possible implications for adsorption isotherm measurements. *Chem. Geol.* **177**, 431–442.

Gautier, J.M., Oelkers, E.H., Schott, J., 2001. Are quartz dissolution rates proportional to B.E.T. surface areas? *Geochim. Cosmochim. Acta* **65**, 1059–1070.

Graustein, W.C., 1981. The effect of forest vegetation on solute acquisition and chemical weathering: a study of the Tesuque Watersheds near Santa Fe, New Mexico. PhD, Yale University.

Graustein, W.C., Cromack, K.J., Sollins, P., 1977. Calcium oxalate: occurrence in soils and effect on nutrient and geochemical cycles. *Science* **198**, 1252–1254.

Hajash, A.J., 1994. Comparison and evaluation of experimental studies on dissolution of minerals by organic acids. In: Pittman, E.D., Lewan, M.D. (Eds.), *Organic Acids in Geological Processes*. Springer-Verlag, Berlin, pp. 201–225.

Harrison, W.J., Thyne, G.D., 1992. Predictions of diagenetic reactions in the presence of organic acids. *Geochim. Cosmochim. Acta* **56**, 565–586.

Harrison, W.J., Thyne, G.D., 1994. Geochemical models of rock–water interaction in the presence of organic acids. In: Lewan, M.D., Prittman, E.D. (Eds.), *Organic Acids in Geological Processes*. Springer-Verlag, Berlin, pp. 355–397.

Huertas, J.F., Chou, L., Wollast, R., 1999. Mechanism of kaolinite dissolution at room temperature and pressure. Part II: kinetic study. *Geochim. Cosmochim. Acta* **63**, 3261–3275.

Kalinowski, B.E., Schweda, P., 1996. Kinetics of muscovite, phlogopite and biotite dissolution and alteration at pH 1–4, room temperature. *Geochim. Cosmochim. Acta* **60**, 367–385.

Kaviratna, H., Pinnavaia, T.J., 1994. Acid hydrolysis of octahedral Mg^{2+} sites in 2:1 layered silicates: an assessment of edge attack and gallery access mechanisms. *Clays Clay Miner.* **42**, 717–723.

Kettler, R.M., Palmer, D.A., Wesolowski, D.J., 1991. Dissociation quotients of oxalic acid in aqueous sodium chloride media to 175 °C. *J. Solution Chem.* **20** (9), 905–927.

Koroleff, F., 1976. Determination of silicon. In: Grasshoff, K. (Ed.), *Methods of Seawater Analysis*. Verlag Chemie, Berlin, pp. 149–158.

Lasaga, A.C., 1981. Rate laws of chemical reactions. In: Lasaga, A.C., Kirkpatrick, J.R. (Eds.), *Kinetics of Geochemical Processes*, vol. 8. Mineralogical Society of America, pp. 1–68.

Lasaga, A.C., 1998. *Kinetic Theory in the Earth Sciences*. Princeton University Press, New Jersey.

Luca, V., MacLachlan, D.J., 1992. Site occupancy in nontronite studied by acid dissolution and Moessbauer spectroscopy. *Clays Clay Miner.* **40**, 1–7.

Metz, V., Ganor, J., 2001. Stirring effect on kaolinite dissolution rate. *Geochim. Cosmochim. Acta* **65** (20), 3475–3490.

Mogollon, J.L., Ganor, J., Soler, J.M., Lasaga, A.C., 1996. Column experiments and the full dissolution rate law of gibbsite. *Am. J. Sci.* **296**, 729–765.

Nagy, K.L., Blum, A.E., Lasaga, A.C., 1991. Dissolution and precipitation kinetics of kaolinite at 80 °C and pH 3: the dependence on solution saturation state. *Am. J. Sci.* **291**, 649–686.

Nagy, K.L., Lasaga, A.C., 1992. Dissolution and precipitation kinetics of gibbsite at 80 °C and pH 3: the dependence on solution saturation state. *Geochim. Cosmochim. Acta* **56**, 3093–3111.

Naumov, G.B., Ryzhenko, B.N., Khodakovsky, I.L., 1974. Handbook of thermodynamic data (translation of Russian report). United States Geological Survey, p. 328.

Novak, I., Cicel, B., 1978. Dissolution of smectites in hydrochloric acid: II. Dissolution rates as a function of crystallochemical composition. *Clays Clay Miner.* **26**, 341–344.

Oelkers, E.H., Schott, J., 1998. Does organic acid adsorption affect alkali-feldspar dissolution rates? *Chem. Geol.* **151**, 235–245.

Oelkers, E.H., Schott, J., Devidal, J.-L., 1994. The effect of aluminum, pH, and chemical affinity on the rates of aluminosilicate dissolution reactions. *Geochim. Cosmochim. Acta* **58** (9), 2011–2024.

Persson, P., Axe, K., 2005. Adsorption of oxalate and malonate at the water–goethite interface: molecular surface speciation from IR spectroscopy. *Geochim. Cosmochim. Acta* **69** (3), 541–552.

Poulson, S.R., Drever, J.I., Stillings, L.L., 1997. Aqueous S-oxalate complexing, oxalate adsorption onto quartz, and the effect of oxalate upon quartz dissolution rates. *Chem. Geol.* **140**, 1–7.

Rufe, E., Hochella, M.F., 1999. Quantitative assessment of reactive surface area of phlogopite during acid dissolution. *Science* **285**, 874–876.

Sposito, G., 1984. *The Surface Chemistry of Soils*. Oxford University Press, Oxford.

Stillings, L.L., Drever, J.I., Poulson, S.R., 1998. Oxalate adsorption at a plagioclase (An47) surface and models for ligand-promoted dissolution. *Environ. Sci. Technol.* **32**, 2856–2864.

Stillings, L.L., Drever, J.I., Poulson, S.R., Brantley, S.L., Yanting, S., Oxburgh, R., 1996. Rates of feldspar dissolution at pH 3–7 with 0–8 mM oxalic acid. *Chem. Geol.* **132**, 79–89.

Stumm, W., 1992. *Chemistry of the Solid–Water Interface: Processes at the Mineral–Water and Particle–Water Interface in Natural Systems*. Wiley, Chichester.

Turpault, M.-P., Trotignon, L., 1994. The dissolution of biotite single crystals in dilute HNO_3 at 24 °C: evidence of an anisotropic corrosion process of micas in acidic solutions. *Geochim. Cosmochim. Acta* **58**, 2761–2775.

van Hees, P.A.W., Lundstrom, U.S., Morth, C.-M., 2002. Dissolution of microcline and labradorite in a forest O horizon extract: the effect of naturally occurring organic acids. *Chem. Geol.* **189**, 199–211.

Walther, J.V., 1996. Relation between rates of aluminosilicate mineral dissolution, pH, temperature, and surface charge. *Am. J. Sci.* **296**, 693–728.

Ward, D.B., Brady, P.V., 1998. Effect of Al and organic acids on the surface chemistry of kaolinite. *Clays Clay Miner.* **46** (4), 453–465.

Welch, S.A., Ullman, W.J., 1993. The effect of organic acids on feldspar dissolution rates and stoichiometry. *Geochim. Cosmochim. Acta* **57**, 2725–2736.

Welch, S.A., Ullman, W.J., 1996. Feldspar dissolution in acidic and organic acid solutions: compositional and pH dependence of dissolution rate. *Geochim. Cosmochim. Acta* **60**, 2939–2948.

Wesolowski, D.J., Palmer, D.A., 1994. Aluminium speciation and equilibria in aqueous solution: V. Gibbsite solubility at 50 °C and pH 3 to 9 in 0.1 molal NaCl solutions, a general model for Al speciation, and analytical methods. *Geochim. Cosmochim. Acta* **58** (14), 2947–2969.

Wieland, E., Stumm, W., 1992. Dissolution kinetics of kaolinite in acidic aqueous solutions at 25 °C. *Geochim. Cosmochim. Acta* **56**, 3339–3355.

Wolery, T.J., 1979. *Calculation of Chemical Equilibrium between Aqueous Solution and Minerals: The eq3/6 Software Package*. Lawrence Livermore Laboratory, p. 41.

Xie, Z., Walther, J.V., 1992. Incongruent dissolution and surface area of kaolinite. *Geochim. Cosmochim. Acta* **56**, 3357–3363.

Yoon, T.H., Johnson, S.B., Musgrave, C.B., Brown, G.E.J., 2004. Adsorption of organic matter at mineral/water interfaces: I. ATR-FTIR spectroscopic and quantum chemical study of oxalate adsorbed at boehmite/water and corundum/water interfaces. *Geochim. Cosmochim. Acta* **68** (22), 4505–4518.